CHALMERS
UNIVERSITY OF TECHNOLOGY

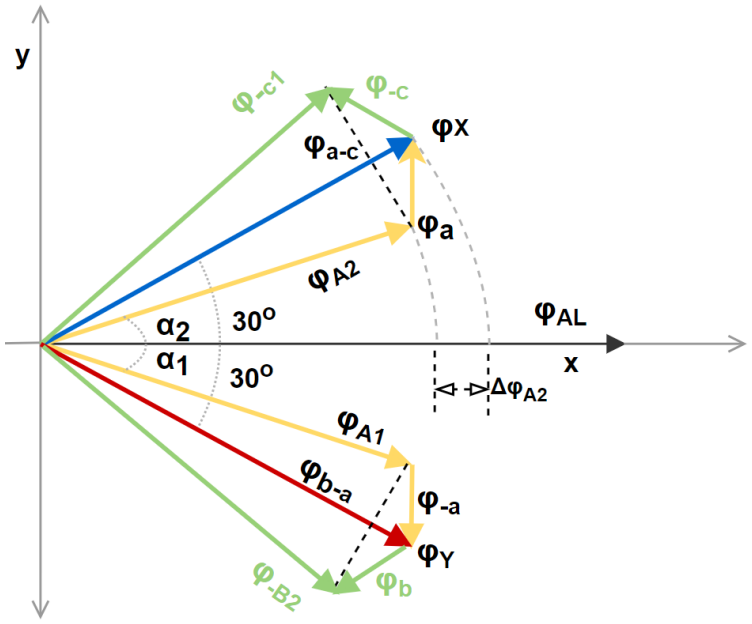

Effects of magnetic bypass on performance of distribution transformers

Master's thesis in Electric Power Engineering

MUNEEB BASHIR CHOUDHRY
MOHSIN UL HASSAN SYED

Department of Electric Power Engineering
CHALMERS UNIVERSITY OF TECHNOLOGY
Gothenburg, Sweden 2019

Master's thesis

Effects of Magnetic Bypass on Performance of Distribution Transformers

MUNEEB BASHIR CHOUDHRY
MOHSIN UL HASSAN SYED

CHALMERS
UNIVERSITY OF TECHNOLOGY

Department of Electric Engineering
Division of Electric Power Engineering
Chalmers University of Technology
Gothenburg, Sweden 2019

Effects of Magnetic Bypass on performance of Distribution Transformers.
MUNEEB BASHIR CHOUDHRY , MOHSIN UL HASSAN SYED

© MUNEEB BASHIR CHOUDHRY, MOHSIN UL HASSAN SYED 2019.

Supervisor: Thomas Türk, Transformer Cage Core AB
Examiner: Yuiry Serdyuk, Department of Electric Engineering, Chalmers University of Technology

Master's Thesis
Department of Electric Engineering
Division of Electric Power Engineering
Chalmers University of Technology
SE-412 96 Gothenburg
Telephone +46 31 772 1000

Cover: vector representation of reduction of loss angle with bypass.

Typeset in LaTeX
Gothenburg, Sweden 2019

Abstract

As the demand for electricity is increasing, the requirement for number of electrical appliances is also increasing. With this increase in number of appliances, the performance criteria for such appliances is also becoming less tolerant. One such important appliance in the power system is distribution transformer. Significant contribution of losses in a distribution transformer is incurred because of no-load losses, if such a transformer is operated at no-load for longer duration then cumulative no-load losses will have a high percentage of total losses. The new EU Commission regulations recommend a further 10 % decrease in the no-load losses by the year 2021.

In this thesis, a prototype of power electronics based active core is developed for a prototype hexa-Core transformer. Since the shape of flux in the winding is sinusoidal and so it follows a hysteresis curve, where magnetic domains are aligned in both of the cycles. The aim was to assist in this change in domain alignment and as a result excitation current from the supply can be reduced, decreasing no-load losses.

The response of this active core was evaluated with fixed DC value for a number of excitation levels in the main core and with fixed excitation in the main core and a number of DC values. Single step grain oriented magnetic bypasses were installed in the core which resulted in the loss reduction of 15% to 19.5% in the main core. This reduction of losses in the core was influenced by the decrease of magnetic flux in the core rings. Furthermore these magnetic bypasses were excited to obtain further loss reduction in the core. This resulted in a further decrease in power loss of approximately 5% depending on the transformer's main excitation and DC value. Further to determine the optimum position for the secondary excitation from DC source the pulse width and firing delay was evaluated.

Another type of wound core transformer the so called evans-core transformer was also tested. The transformer showed similar behaviour to that of hexa-core. Different bypass strategies were also evaluated and a decrease in excitation losses was achieved with these bypass strategies.

Keywords: Hexa-core Transformer, Transformer losses, Magnetic Bypass, Active Core Control, Evan's Core, Hexa-core, Single step bypass, Evans core.

Acronyms

CSA	Cross-sectional area
EGO-1	Evans-core grain oriented bypass 1
EGO-2	Evans-core grain oriented bypass 2
EGO-3	Evans-core grain oriented bypass 3
ϕ_a	Flux in bypass
ϕ_A	Flux in leg A
ϕ_B	Flux in leg B
ϕ_C	Flux in leg C
A1	Inner Core ring 1
A2	Inner Core ring 2
α	Loss Angle
SPWM	Sinusoidal Pulse Width Modulation
W_A	Winding on leg A of Evan's core transformer
W_B	Winding on leg B of Evan's core transformer
W_C	Winding on leg C of Evan's core transformer
W_1	Winding on leg 1 of Hexa-core transformer
W_2	Winding on leg 2 of Hexa-core transformer
W_3	Winding on leg 3 of Hexa-core transformer
y_a	yoke between winding 1 and winding 2
y_b	yoke between winding 2 and winding 3
y_c	yoke between winding 1 and winding 3

Acknowledgements

Authors would like to thanks ALLAH Almighty for giving us the will and strength to complete this thesis work. Authors would also like to thank and pay sincere gratitude to Yuiry Serdyuk, supervisor and examiner of this project, for his guidance and great support throughout the thesis work. His motivation, dedication and expertise has helped us in achieving this goal and successfully completing our thesis work.

Authors would also acknowledge the efforts of Thomas Türk, supervisor at Transformer Cage Core AB and would also like to thank him for his motivation and guidance towards this project work. His ideas has helped us throughout the thesis work.

Authors would also like to express their sincere gratitude to everyone at the Division of Electric Power Engineering for their help and guidance, esp. Haider Ali and Douglas Nilsson, in completing this work.

Authors would also like to thank their families and friends for their love and support throughout the whole studies.

Muneeb Bashir Choudhry, Gothenburg, October 2019

Mohsin Ul Hassan Syed, Gothenburg, October 2019

Contents

List of Figures

List of Tables

1
Introduction

1.1 Background

As the demand for electricity is increasing, the requirement of number of electrical appliances is also increasing. With this increase in number of appliances the performance criteria for such appliances is also becoming less tolerant. One such important appliance in the power system is distribution transformer. Distribution transformers are utilized in transfer of energy from the main feeder to the customer end. Since the loads connected to these transformers are critical therefore the performance criteria for such transformers is very strict both in terms of reliability and efficiency.

To overcome the increased energy demand, one solution, though not a cheaper solution, is to generate more electric power but according to **EU** regulations, the gross electricity generation in **EU** between year 2005 and 2016 has decreased by 2 % by an average rate of 0.2 % annually. During the past 9 years, it kept on decreasing by the decreasing rate of 0.6 % [**1**]. The other solution is to overcome or reduce the losses during transmission and distribution. The later solution is much cheaper solution. One major contribution of losses in a distribution transformer is incurred because of no-load losses, as these transformers operates mostly on no load. The new EU regulations recommend a further 10% decrease in the no-load losses by 2021.

Iron losses and Copper losses are the two major constituents of these losses [**2**]. No-load losses can be decreased by using more iron in the core material to increase the cross section area of the leg to take down the induction level. But this additional amount of iron to be added results in a more expensive core since the amount of the winding material also must increase, so studies are now being carried out to suggest an alternative which avoids adding more winding material to the core.

1.2 Problem description

It has been experimentally established that using a symmetric magnetic bypass strategy on a hexa-core transformer can significantly reduce the no-load losses [**3**]. Now the motivation is to evaluate if the bypass strategy can be applied on another wound core geometry called Evans-core. Another theory suggests that by introducing a dynamic control of the magnetic domains in the core material can result in further decrease in magnetization current resulting in further reduction of magnetization

losses in the transformer.

1.3 Aim

The aim of this thesis is to evaluate the decrease in losses on an Evans-core using different bypass strategies. The investigation regarding possibility to control the amount, phase, and shape of magnetic flux in the bypass by feeding and controlling current in auxiliary windings applied on the bypasses is also investigated in the thesis.

1.4 Scope

This thesis work has to be carried out in two phases. During the first phase, the active flux control will be implemented on the Hexa-Core transformer in order to control the shape and phase of magnetic flux and calculate how much losses are reduced. In the second phase, it will be investigated how much losses are reduced in a prototype of an Evans core by introducing magnetic bypass. The terms excitation level, induction level and magnetic field strength etc. are interchangeably used in this thesis to refer to the excitation level in the transformer.

1.5 Limitations

As the windings for the transformer core will be hand wound, so there might be some uncertainties in the measurements due to deformation or non-uniformity of airgaps. As it is established by earlier studies on this transformer that there was a manufacturing defect in the transformer's core and the core is highly unbalanced so this can also lead to the variation in the measured values and theoretical results. Further it is to be noted that due to the limitation in availability of the material the bypasses are implemented on one side of the Evans-core transformer, therefore reduction in losses can be higher if these bypasses are implemented on both sides of the Evans-core transformer.

1.6 Ethics and sustainable aspects of the project

Since the aim of this project is optimum utilization of the energy, therefore it can have a long standing impact on sustainability. With optimum utilization of energy, there will be a decrease in production demand which in return can be helpful in reduction of usage of carbon fuel and impact of non environment friendly generation. In this project the data to be reported has to be measured and then reported therefore it demands great deal of academic ethics to publish the results as per actual. Since the experimental part of project consists of working on live wires and high voltage, therefore special attention should be paid to safety precautions.

2

Transformer

Transformer is an electrical machine analogous to a stationary induction machine used to transform electrical energy either from high voltage level to low voltage level (step-down) or from low voltage level to high voltage level (step-up) [**4**]. Step-up or transmission transformers are used at the generating units in order to increase the voltage level so that power could be transferred to far distances with lower losses. On the other hand, step down or distribution transformers are used at the consumer/load end and ranges form few hundred volts to few kilo-volts (kV). In such distribution transformers a significant amount of power is wasted in the excitation of the core.

This chapter discusses the working principle of power transformers and different core types and materials used in transformer's designing. It also focuses on different types of losses which exist in transformers during operation.

2.1 Working principle of transformer

Transformer works on the principle of electromagnetic induction, also known as Faraday's law of induction, which describes that how a varying magnetic flux in a coil induces voltage in it. Fig. 2.1 depicts a coupled/mutual flux between primary and secondary windings of transformer. The transformer consists of a magnetic core upon which windings are wound. Core is usually made up of thin and laminated steel sheets and are stacked over each other to provide desired cross section area of the core legs [**5**]. Magnetic core provides a path for the flux to flow and insulation layers upon the sheets helps reduce the eddy currents in the core. The alternating current in the primary windings produces a varying magnetic flux which passes through the magnetic core and induces a varying electromotive force emf in the secondary windings due to electromagnetic induction. A varying current starts to build up at the secondary windings which in turn produces a flux of equal magnitude as in primary but opposite in direction. This flux opposes the flux produced by the primary windings according to Lenz's law.

The ratio of number of turns in the secondary and the primary windings dictate the voltage level. Higher the number of turns at output, higher will be the output voltage level.

According to Faraday's law, the arbitrary voltage at either sides of the transformer

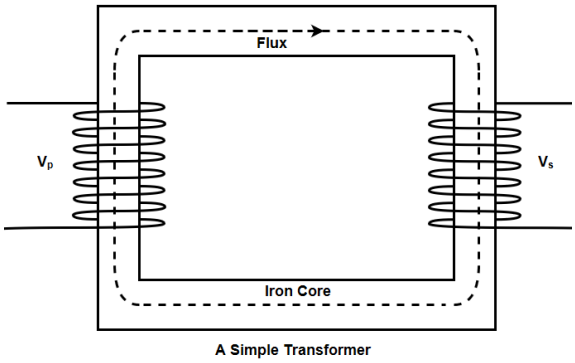

Figure 2.1: A simple transformer

at any time can be given by equations (2.1) and (2.2) as

$$v_p = N_p \frac{-d\phi}{dt} \tag{2.1}$$

$$v_s = N_s \frac{-d\phi}{dt} \tag{2.2}$$

whereas ϕ is the flux in the magnetic core. From equations (2.1) and (2.2), a relation between voltages and number of turns at either sides of the transformer can be derived and is represented as their respective phasors in equation (2.3) as

$$\frac{V_s}{V_p} = \frac{N_s}{N_p} \tag{2.3}$$

where V_p and N_p represent the voltage and number of turns at primary respectively and V_s and N_s represent the voltage and number of turns at the secondary side respectively .

$$V_p I_p = V_s I_s \tag{2.4}$$

In an ideal transformer, keeping the power same at both ends, the current transformation can be derived by using equations 2.3 and 2.4 as

$$\frac{I_s}{I_p} = \frac{N_p}{N_s} \tag{2.5}$$

where as I_p and I_s represent the primary and secondary currents respectively. The equations (2.3) and (2.5) holds for any alternating voltages and currents respectively. These equations are also valid if a transformer would be energized with an alternating, sinusoidal voltage. Assume a sinusoidal voltage is applied at the primary end of the transformer. This voltage is given by equation (2.6)

$$v_p = \sqrt{2}\ V_p\ sin\ \omega t \tag{2.6}$$

Equations (2.1) and (2.6) yields the time dependent flux rate in the core

$$\frac{d\phi}{dt} = \frac{\sqrt{2}\ V_p}{N_p}\ sin\ \omega t \tag{2.7}$$

The flux in the core will be given by integrating equation (2.7). The maximum core flux is given by equation (2.8)

$$\Phi_{max} = \frac{\sqrt{2}\ V_p}{\omega\ N_p} = B_{max} \cdot\ A \tag{2.8}$$

where as B_{max} is the maximum magnetic flux density and A is the cross-sectional area of the magnetic core.
The current in the primary winding produces a magnetic field according to amperes law. The iron core provides a low reluctance path for the flux to move and this flux interacts with secondary winding and induces emf in the secondary winding. From equation (2.8), the voltage at the either sides of the transformer can be written as a generic expression in (2.9)

$$V = \sqrt{2}\pi f N A B_{max} \tag{2.9}$$

where f is the electrical frequency and N is the number of turns on either sides, B_{max} is the magnetic induction level for the given cross sectional area of the core. Equation (2.9) for a given distribution system can also be represented as

$$V \propto N A B_{max} \tag{2.10}$$

2.2 Transformer Core & Material

Transformer core is one of the most important thing when it comes to designing a transformer. The efficiency of the transformer is influenced also by the design of the core. Transformer core is usually made of thin sheets of ferromagnetic material stacked over each other to get the required thickness. The reason for using thin sheets is to help reduce eddy current losses in the core. There are various types of transformer core designs depending upon the function and type of transformer. It could be E type, E-I type etc. According to previous studies on performance of distribution transformers, it has been established that a symmetrical shape of transformer core helps in reducing losses in the core. In this project, a hexa-core transformer and an Evan's core transformer were tested for no-load losses. Further a control strategy was developed for hexa-core to reduce no-load losses. In the following sections, two types of cores will be discussed.

2.2.1 Hexa-core transformer

Hexa-core transformer is a type 3 phase symmetrical core transformer. Its three core legs are symmetrically placed at 60° apart from each other similar to a equilateral triangle. To have a clear picture of hexa-core transformer, it can be imagined as an equilateral triangle box of certain height and then putting the windings on the the corner of the triangle. The top view of the hexa-core transformer is illustrated in Fig. 2.2 where W_1, W_2, and W_3 represent the three individual windings on the respective limbs and y_A, y_B and y_C represent the yoke between respective windings. These core rings are formed by making frame like loops, which contains thin layers

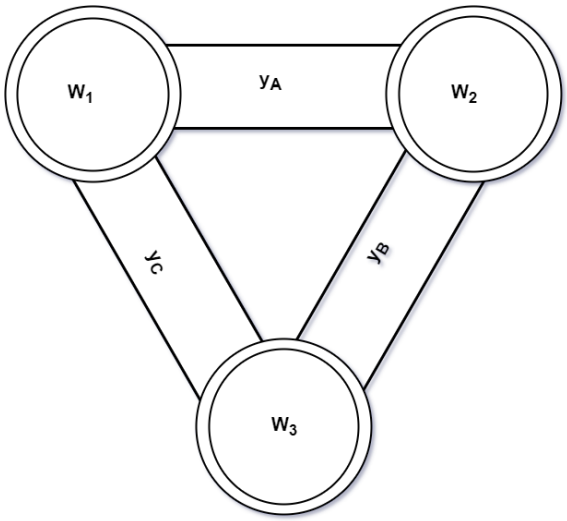

Figure 2.2: Illustration of top view of hexa-core transformer

of steel stacked on each other.
The vertical sections of the magnetic core are the limbs which can also be referred to as legs on which the windings are wound. The horizontal sections (top and bottom) of the magnetic core the yokes.

The core of hexa-core transformer is made up of nine rolls of steel sheets and the symmetrical core legs illustrates a hexagonal structure thus known as Hexaformer or Hexa-core transformer [**5**]. This kind of symmetrical core shape has revolutionized the distribution transformers and has a lot more benefits over traditional E-type core. The hexa-core transformers have higher energy efficiency, lower reluctance than E-type due to symmetrical shape, lower weight & volume and lower electromagnetic stray field [**5**].

2.2.2 Evans-core transformer

Evans core transformer is another kind of transformer being developed for increased efficiency along with the reduction in core losses (no-load losses). It is similar to the hexa-core transformer in arrangement. It has three individual core rings made of wound steel of which two rings are identical. The two identical core rings with equal mean path are smaller in dimensions than the outer bigger core ring and are fitted inside it. Fig. 2.3 illustrates the shape and structure of a three phase Evan's core transformer. The two identical core rings are fitted inside the outer core ring and every phase winding always shares two legs of individual core rings. Similar to hexa-core transformer, these windings also have an equal cross sectional area of limbs [**5**].

2.2.3 Ferromagnetic material

Ferromagnetism is the materialistic property of certain materials, which is either exhibition of strong attractive forces to become a permanent magnet or to show

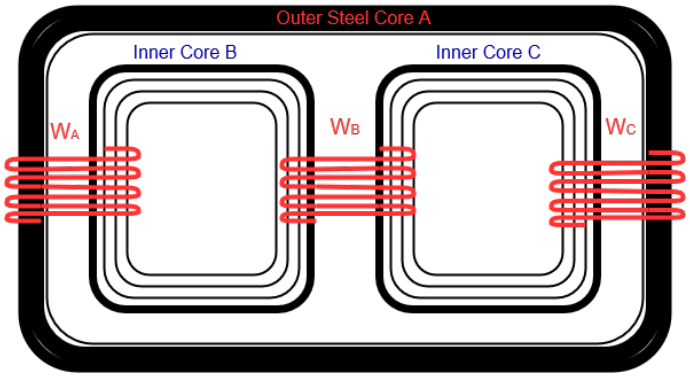

Figure 2.3: Illustration of Evan's core transformer

attraction towards other magnetic materials. Ferromagnetic materials exhibit long range alignment phenomenon when in the presence of external magnetic field [**6**] and electrons movement is aligned with each other in a region also known as magnetic domains. These domains are highly influenced by the strong magnetic fields and material is said to be magnetized. Ferromagnetic material also exhibit memory property of remembering the magnetic domain which is known as hysteresis property in which material under the influence of magnetic field follows the domain called as "Hysteresis loop" which is illustrated in Fig. 2.5.

2.3 Losses in transformer

There is not any electrical operating device without any losses. There are different reasons behind these losses. As transformer is analogous to a static induction machine, unlike induction machine it does not exhibit frictional or rotational losses [**7**]. Anyhow there are four different types of losses that exist in the transformer during operation and these will be discussed here. These are iron core losses, copper losses, stray losses and dielectric losses. Most of the losses comprises of core and ohmic losses. In this thesis work, stray and dielectric losses were considered to be negligible. The following Fig. 2.4 shows the breakdown of different losses in the transformer.

2.3.1 Iron core losses

As the name suggests, these losses exhibit in the core of the transformer when it is in operation. These loses constitute a significant part in overall losses of a distribution transformer. There are two major types of iron core losses, hysteresis losses and eddy current losses. These losses are defined in the following subsections.

2.3.1.1 Eddy current losses

When a transformer core is exposed to an alternating magnetic flux, it induces an emf in the core due to magnetic induction. As the transformer core is made up of a ferromagnetic material, (a conducting material in itself) it allows the current to

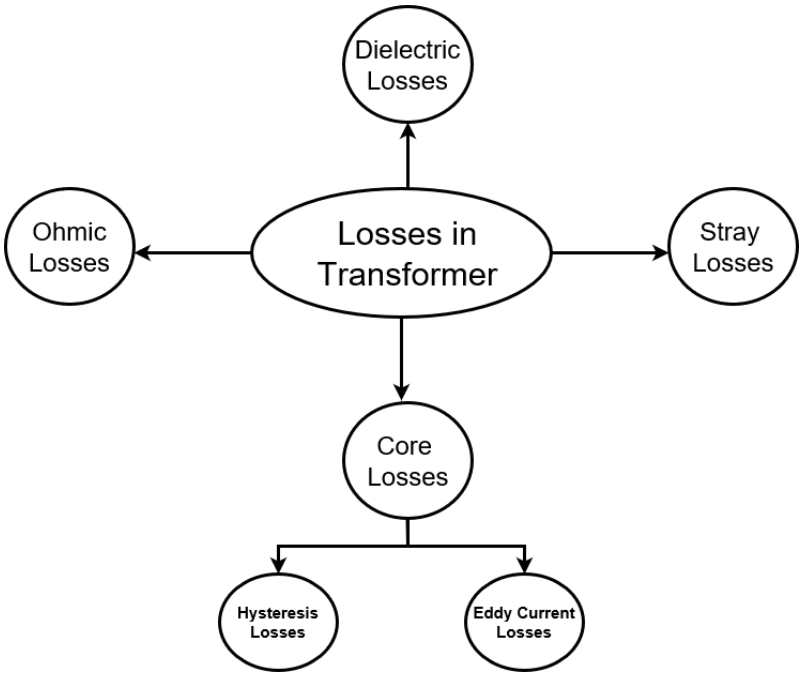

Figure 2.4: Breakdown of losses in a transformer

circulate over the surface of the steel sheets which are parallel to each other. These circulating currents are called eddy currents and thus produces heating losses in the transformer. Eddy current losses depend upon various factors e.g., type of magnetic material, volume of the material etc., but are mainly influenced by the rate of change of flux and path resistance [3]. The eddy current losses can be represented by the following equation

$$P_e = k_e V f^2 B_{max} t^2 \tag{2.11}$$

where k_e is the magnetic material dependent eddy current coefficient, t is the thickness of lamination, V is the volume of the magnetic core and f is the magnetic frequency (number of completed magnetic cycles per second) [3].

2.3.1.2 Hysteresis losses

Hysteresis is the property of the magnetic material and it happens during magnetization and demagnetization of the magnetic material. It happens during the magnetic field reversal phenomenon in which the current changes its polarity and thus in result it magnetizes the core during either current flow and demagnetizes the core during the opposite current flow.

When a magnetic field is applied on the magnetic material, the magnetic particles tries to align themselves in the direction of magnetic field. During the instant of magnetic field reversal, the already aligned magnetic particles resists the change in the direction and thus magnetic energy is lost in order overcome this undue resistance from the magnetic particles to align them back to complete the loop. This loss of energy produces heat known as hysteresis losses **[9]**.

$$P_h = k_h f B_{max}^{\beta} \tag{2.12}$$

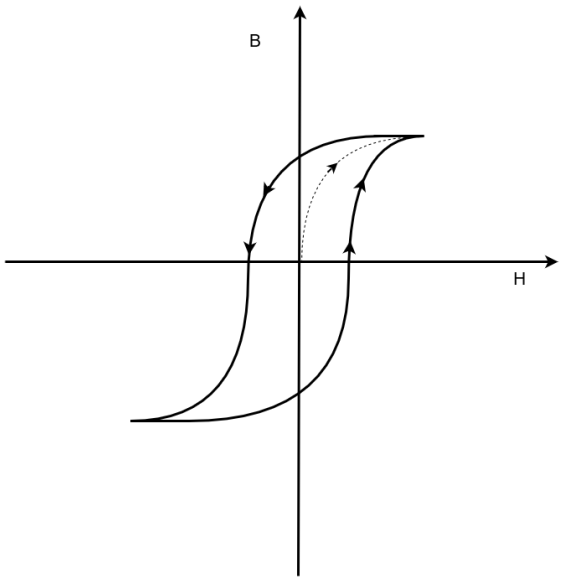

Figure 2.5: An illustration of hysteresis loop for a ferromagnetic material

The equation (2.12) represents the hysteresis losses in any ferromagnetic material where k_h is the hysteresis coefficient and β is the power of B_{max} [5]. The illustration of hysteresis loop of a ferromagnetic material is shown in Fig. 2.5.

2.3.2 Copper losses

Copper losses in the transformer are due to the ohmic resistance of the copper windings. These losses are generally load dependent as the change in load have significant effect on the current drawn from the transformer and according to the equation (2.13), copper losses increases by the square of current **[10]**. Copper losses also depends upon the number of turns as resistance changes with the increase in length ($R \propto L$) so copper losses at the primary and secondary side may be different from each other due to different number of turns but the total losses would be the sum of both. Copper losses increases the temperature of the transformer hence reducing the overall efficiency of the transformer.

$$P_{cu} = I^2 R \tag{2.13}$$

2.3.3 Stray and Dielectric losses

Stray losses in transformer are due to the presence of leakage magnetic field. These losses are very low and can be neglected. Other losses in the transformer are due to the dielectric characteristics of the insulation material used. Dielectric being used in transformer insulation are vulnerable to electric fields and thus deteriorates resulting in partial discharges which further deteriorates the insulation and causes heating losses in the transformer **[8]**.

3

Bypass

Both hexa-core and Evans-core are wound cores. The wound cores do not have the corner joints and air gaps, which is advantageous in comparison to the stacked E-cores. In case of E-cores these corner joints and air gaps increase the building factor.

As a down side, 50 % of the cross-section area in one leg gives static flux path (the core ring) to one of the other legs and the other 50 % of the cross-section area gives static flux path to the third leg. Hence resulting in the flux to be locked in one core ring with little or no possibilities for flux interchange with the other core rings. This will force a phase shift of the flux in the core rings by ca $\pm 30°$ with reference to the common flux in the leg as seen in Fig. 3.2. As a result the flux amplitude in the core rings will increase with ca 15 % $(2/\sqrt{3})$ and the resulting losses will increase with ca 30% $((2/\sqrt{3})^2 \approx 1.33)$ which is the typical building factor for a wound core. With bypass we can introduce new flux paths for enabling flux to leave one core ring and enter another. This takes down the forced phase shift and thus the losses in the core, i.e. the building factor is reduced.

3.1 Types of Bypass configuration for Hexa-Core

As discussed earlier, there are three different bypass configurations for this transformer. These configurations depends upon the angle between the yoke and the bypass which enables the flux to pass in two or more jumps rather than single jump of 120 degrees [**11**]. These configurations are described below.

3.1.1 Single step

In this configuration, a thin laminated steel sheet was placed between the two limbs which makes an adjacent angle of 60° between bypass and the limb. The flux takes 120° shift in two jumps of each 60°.

3.1.2 Two steps

In this configuration, two thin laminated steel sheet were placed between the two limbs which makes an adjacent angle of 40° between bypass and the limb. The flux takes 120° shift in three jumps of each 40°.

3.1.3 Three steps

In this configuration, two thin laminated steel sheet were placed between the two limbs which makes an adjacent angle of 20° between bypass and the limb. In addition to that, a triangular sheet is placed between these two sheets making an angle of 40° with them. The flux takes 120° shift in four steps of which 20° shift between limb and sheet and 40° each between sheet and triangular plate.

3.1.4 Influence of bypasses on magnetic circuit and losses

As previously discussed, the above mentioned three bypass arrangements were evaluated on the hexa-core transformer during the previous thesis work. It has already been established that all of the above mentioned bypasses resulted in reduction of losses, but the three step bypass yielded the maximum reduction in loss [**3**].

The flux distribution inside a hexa-core transformer without bypasses is shown in Fig. 3.1. It can be seen that the main windings for the hexa-core transformer are at 120° apart from each other. So the flux between two phases is 120° apart.

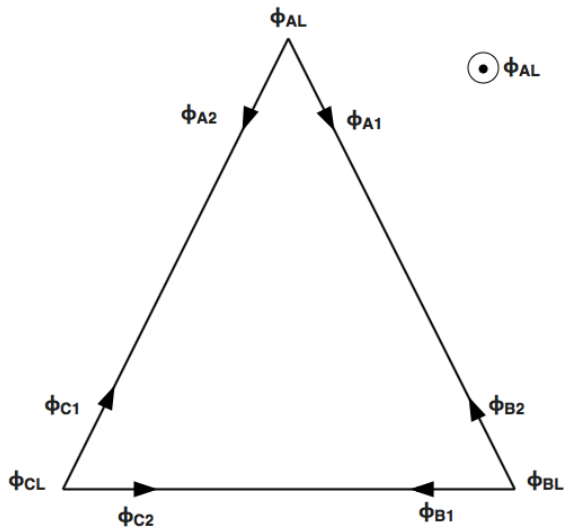

Figure 3.1: Flux orientation in a hexa-core transformer without bypasses

Further due to the construction the flux in each leg is divided into two constituents. The constituents A1 and A2 have flux vectors which are 60° apart from each other. The resultant vector diagram for one phase is illustrated in the Fig. 3.2, where α is defined as the loss angle.

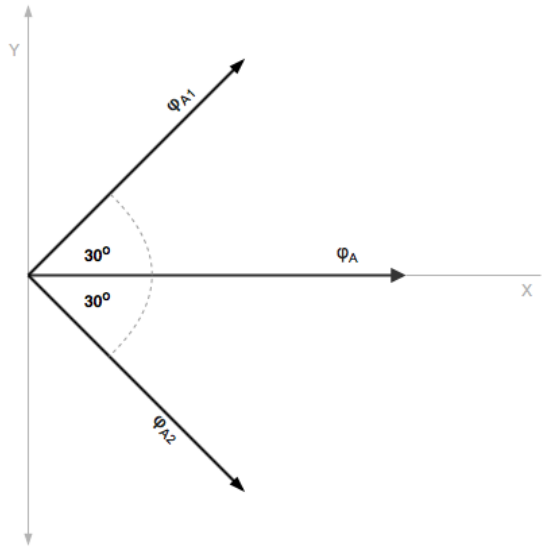

Figure 3.2: Vector representation of flux in one phase of hexa-core transformer

With introduction of bypasses in the core, the main aim is to reduce this angle. The reduction in this angle results in the reduction of losses. An illustration of flux distribution in the transformer with introduction of bypasses is show in the Fig. 3.3 where ϕ_A is the main flux in leg A.

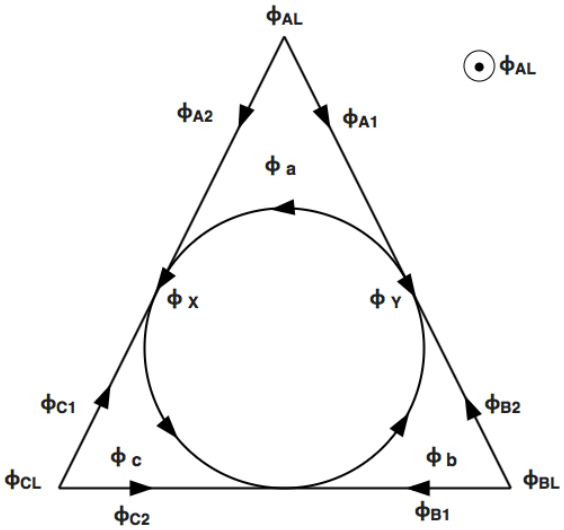

Figure 3.3: Flux orientation in a hexa-core transformer with bypasses

Applying Kirchoff's current law to the magnetic circuit shown in above Fig.3.3, following equations can be derived as:

$$\vec{\phi_c} = \vec{\phi_{A_2}} + \vec{\phi_{C_1}} + \vec{\phi_a} \tag{3.1}$$

$$\vec{\phi_a} = \vec{\phi_{A_1}} + \vec{\phi_{B_2}} + \vec{\phi_b} \tag{3.2}$$

$$\vec{\phi_b} = \vec{\phi_{C_2}} + \vec{\phi_{B_1}} + \vec{\phi_c} \tag{3.3}$$

Solving the above set of equations for phase A yields,

$$\vec{\phi_{A_2}} = \vec{\phi_c} - \vec{\phi_{C_1}} - \vec{\phi_a} \tag{3.4}$$

$$\vec{\phi_{A_1}} = \vec{\phi_a} - \vec{\phi_{B_2}} - \vec{\phi_b} \tag{3.5}$$

From the above equations it can be inferred that with inclusion of the bypasses the flux through the two core rings A1 and A2 decreases which results in a reduction of the projection of the two vectors on main flux. This reduction of projection results in a decrease of loss angle α. This vector representation is illustrated further in the Fig.3.4 illustrates the flux distribution in core after introducing bypass. The figure illustrates the flux vectors and loss angle α for phase A. The remaining vectors are symmetrical to phase A, but only 120° apart. Fig. 3.4.

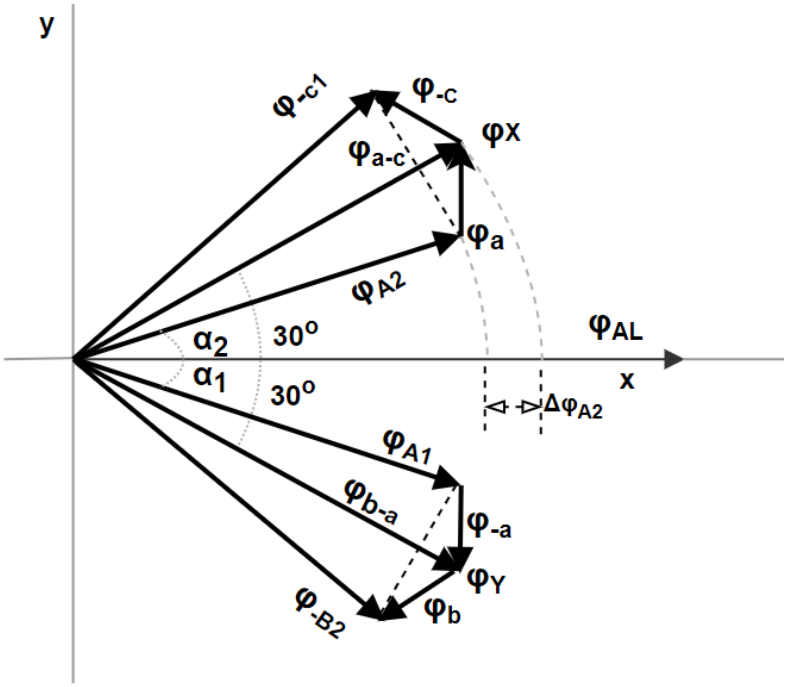

Figure 3.4: Vector representation of flux with introduction of bypass

3.2 Types of Bypass configuration for Evans Core

There were several bypass configuration which can help reduce power losses in distribution transformers at no-load. But in this thesis, only three configurations were used and their effect on loss reduction was analyzed. All the bypass configurations part used were of Grain Oriented Steel and similar thickness as of the transformer core individual sheets itself. There is not any specific name for the configuration, so configurations are named according to type and a numeric suffix for the ease to differentiate between them.
To construct the bypass configuration, two pieces each of bypass piece 1 or 2 depending upon the bypass configuration were inserted between two layers of lower

core ring and two layers from the outer core ring correspondingly. Two pieces of bypass were inserted between the two slits. The idea behind this double layer bypass configuration is that it is faster to install. The illustration of how flux changes direction is given in Fig. 3.5.

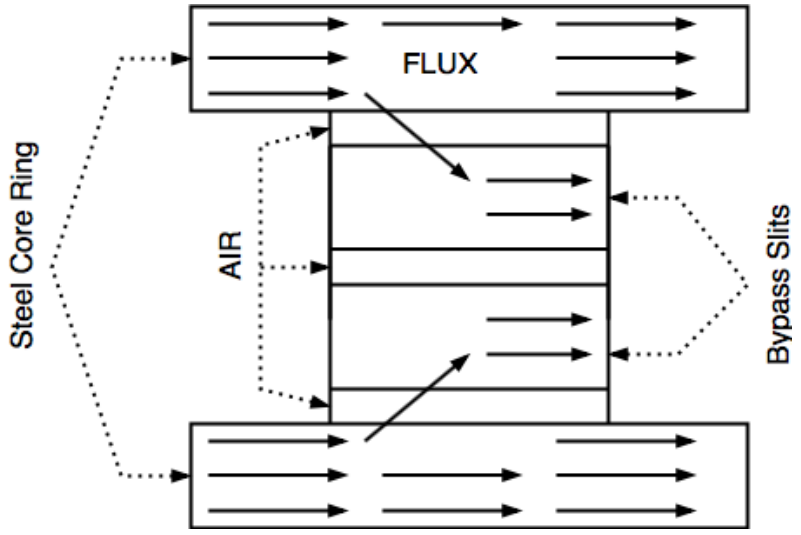

Figure 3.5: Orientation of flux in core and bypass

In Fig. 3.5, two bypass pieces were placed between the two successive core rings/sheets. The arrow shows the direction of the flow of flux. By the introduction of bypass, some amount of the flux flowing in the core rings, corresponding to the cross sectional area of the bypass, starts flowing through the bypasses.

The Fig.3.6 is the first configuration of bypass and is named as configuration "EGO-1". This bypass configuration was constructed with four different types of bypass pieces for deflecting flux in the core rings. This bypass configuration consisted of three sub-bypass configurations i.e., B1, B2 and B3. B1,the right most configuration in Fig.3.6 for deflecting flux from lower core ring "C" to outer core ring "A" and the B2 responsible for deflecting the flux from core ring "A" to the third core ring "B". The B2 is responsible for bypassing flux between "B" and "C". Two five sided polygon bypass pieces,on each side, between two successive core sheets and two pieces between them deflects the flux from lower to upper or the other way around in 4 steps each.

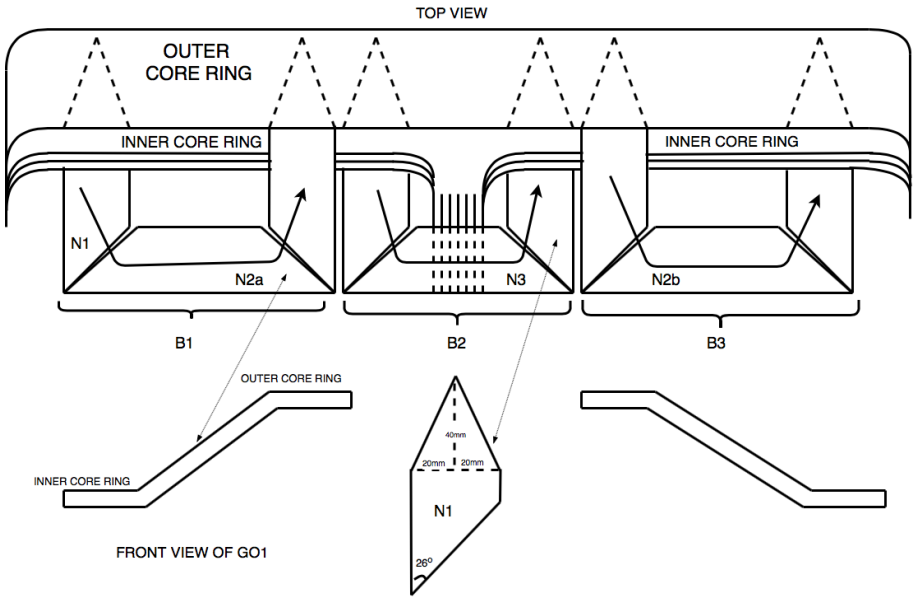

Figure 3.6: Configuration of EGO-1

The Fig.3.7 is the second configuration of bypass and is named as configuration "EGO-2". This bypass has the similar architecture as of the EGO-1 but the width of bypass pieces is changed. In this configuration, the width of new bypass piece was increased by 50% as of that used in previous configuration. The bypass piece was wider in order to increase the cross section are of the bypass.

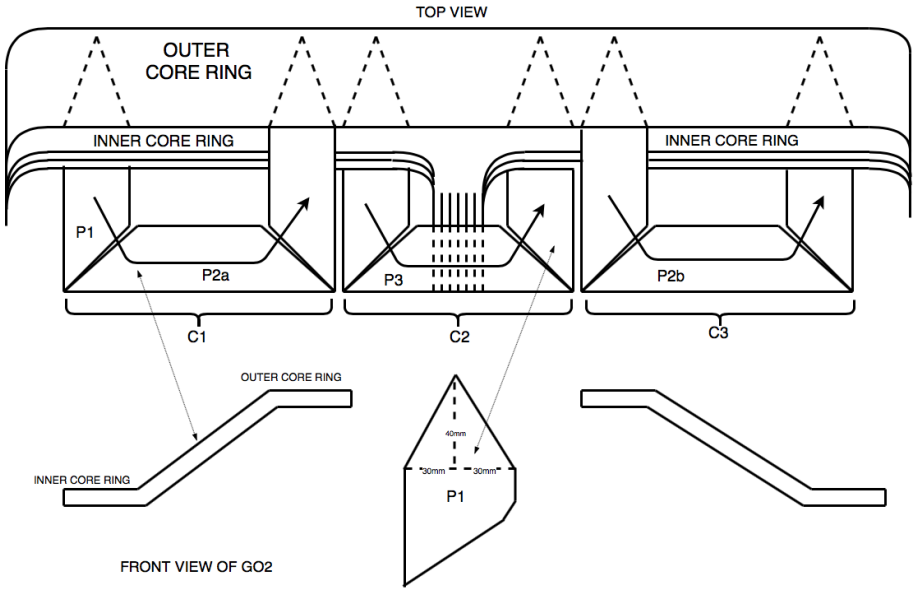

Figure 3.7: Configuration of EGO-2

The third type of bypass configuration used was different from the previously described configurations. This configuration was named as "EGO-3" in which the flux from the outer ring was shifted to a common piece connecting both the inner rings.In Fig.3.8 this common piece is named N4. Same bypass piece as of the EGO-2 configuration, was used in this configuration. Further a U-shaped piece with triangular

faces on both sides was used to make a path for flux to flow from outer yoke to the inner yokes. This configuration uses lesser material and has lower bypass to core ration as compared to the other two configurations. The comparison of these three configurations as per different parameters and their effect on loss reduction are discussed in later chapter. The EGO-3 configuration is shown in Fig.3.8.

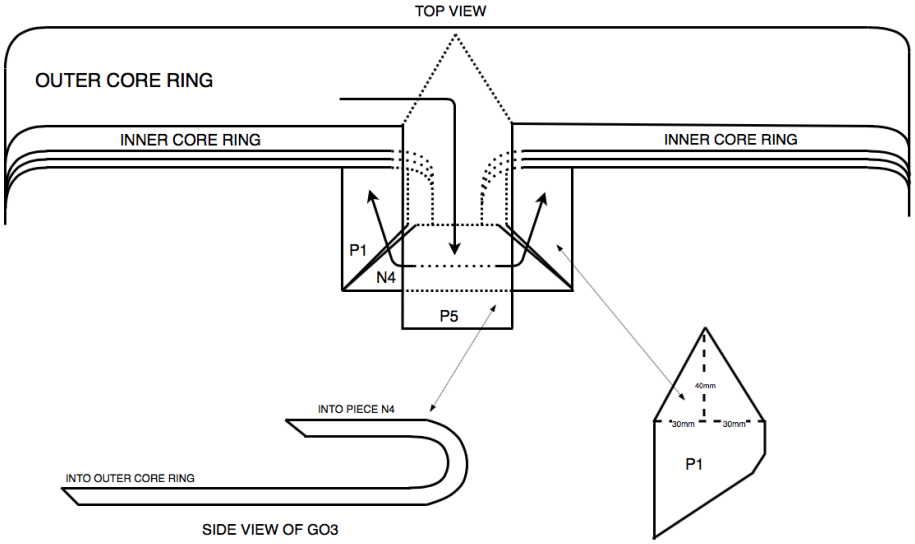

Figure 3.8: Configuration of EGO-3

4

Methodology

In this chapter, the approach taken to carry out project is presented. This thesis work is carried out in a structured approach. Further a brief description of each stage is provided in the following sections.

4.1 Literature Review

The thesis started with intensive literature review. Since this thesis was based on an innovative idea of development of a prototype therefore searching for the relevant literature was challenging. However since work was previously done on such type of a core, this provided a good starting point. Further different research papers and journals were consulted for general behaviour of magnetic circuit and relevant deductions were made about the shape of flux under the power electronics circuitry.

4.2 Experimental Setup

To evaluate the response of the magnetic core following properties were important to examine:

- Flux in the core leg.
- Input power to no-load transformer
- Flux in the bypass.

Flux in the main winding is crucial to examine the magnetic circuit of the transformer and inter-dependence and orientation of the flux inside the core.
Where as, since the transformer is operating on no load condition therefore the input power constitutes the excitation losses.
For this a setup for measurement of these quantities was devised which is further described in the next chapter.

4.3 Reference measurement

To begin with the reference measurement for the core was taken and verified against the values obtained through previous studies. This was done to ensure the core still retains its magnetic properties. This was also done to verify the measurement setup used for the measurement of losses.

Figure 4.1: Master thesis timeline

4.4 Power Electronic Circuit Development

Power electronics development was started with intensive literature studies. Once the required configuration for the converter was determined, various components to be used in such a converter were studied. Depending on the mode of operation a complimentary configuration of converter was developed.

4.5 Evans Core measurement

Evans core as described in previous chapter like the Hexa-core is a wound core. Therefore the behaviour of two cores is some what similar. However to establish a reference working initially the Evans core was energized without any bypasses and a reference loss curve was established. This reference loss curve provided excitation losses against a range of operating flux in the main core. Later different types of bypass arrangements were installed in the transformer and the results were compared to previously established reference curve.

4.6 Data Acquisition & Analysis

After performing the practical measurement on the designed system, results were obtained. The obtained results are presented in the coming chapters. The results are one dimensional interpolated to have a smoother curve, which in return helps in predicting the behaviour of core through various data sets.

5

Measurement setup

For the analysis of both transformers, a measurement setup was developed. This chapter focuses on the different measurement techniques used for measuring flux in the core. Furthermore a so called active core control setup was developed to excite the bypasses in order to reduce losses in the main core. Different measurement equipment used during thesis are also discussed later in this chapter.

5.1 Transformer core

Transformer core used in this thesis was a down-scaled prototype of Evans core. The core was made of M4-Oriented Carlite steel sheets of 0.27 mm thickness of steel. The outer core was made by stacking 24 such steel sheets and the inner two cores consisted of 23 steel sheets each. The transformer core was constructed with 1.0 mm wide slits (airgaps) between each two pair of steel sheets in the yoke in order to able to adjust bypass pieces into the yokes. The physical specification of transformer core and material specifications, provided by the manufacturer, are given in Tab. 5.1

Physical Specifications of Evans core		
Specifications	Unit	Quantity
Width of steel sheet	mm	40
Thickness of steel sheet	mm	0.27
Volume of the core	dm^3	23.43
Density of Iron	Kg/m^3	6.37
Weight of the core	Kg	8.41
Number of outer sheets	-	24
Number of inner sheets	-	23
Stacking factor	-	0.97
Cross-sectional area of leg	mm^2	492.37

Table 5.1: Physical specification of Evans core

5.2 Core windings

There were two criterion for choosing the core windings. First criteria was the peak currents through the winding during the region of high saturation. Magneto motive

force mmf is the quantity, analogous to voltage in electric circuits, which gives rise to magnetic fields. It depends upon the mean path length L and number of turns of the coil N, magnetic flux Φ, the magnetic resistance to the field called as reluctance $\Re$ and the current through the coil I. By equating magneto motive force F for magnetic intensity H and current in N turns of the coil, the high peak current in the winding can be calculated as:

$$I = \frac{HL}{N} \tag{5.1}$$

It is a common practice to test distribution transformers at magnetic induction of 1.7 T or more. So in this thesis, measurements were being taken at 2.2 T as well, so the maximum peak current was estimated according to 2.0 T. By using equation 5.1, the peak current in the winding was found to be 11.82 A, so in order to withstand such high current, a copper wire of diameter 3.5 mm was selected which has very low resistance of 0.016 Ω per winding comprising of 120 turn each. Mean length of each winding was 24 meters. Such low resistance contributes to less than 1% copper losses in the winding even at the hard saturation region where magnetic induction intensity is higher than 2.2 T, copper losses were less than 3.04 %. The selected wire can also withstand high currents up to 50 A. Second criteria was to decide the number of turns for each winding which in results dictates the magnetic flux flowing through them. For such high voltages and magnetic induction, the number of turns were decided to be 120 turns in total, three layers of 40 turns each were wound on each leg.

5.3 RC integrator

To measure the flux magnitude in the core leg and bypasses, a so called low pass filter was designed. This low pass filter is an RC integrator circuit with a feeding voltage from the search coil. It attenuates the higher frequencies which are usually in form of noise, and allows the low frequencies to pass.
Ideally such a filter, should have the components in such a way that:

$$\omega >> \frac{1}{RC} \tag{5.2}$$

where as $\omega = 2\pi f$. In principle at higher frequencies the capacitive reactance X_c is quite low, where as it is very high as compared to the resistance at lower frequencies. Having a lower capacitive reactance results in a negligible voltage drop on capacitor.

Since voltage across capacitor is proportional to the flux in the search coil, therefore it gives a decent idea of shape and strength of magnetic flux inside the search coil.

The values for components in circuit implemented were chosen to be 470 nF and 100 Ω. Since it is a low pass filter so it tends to add a phase shift in the output circuit which in case of implemented circuit was calculated to be 1.67°. The value for phase shift is quite small there for it can be neglected in this application.

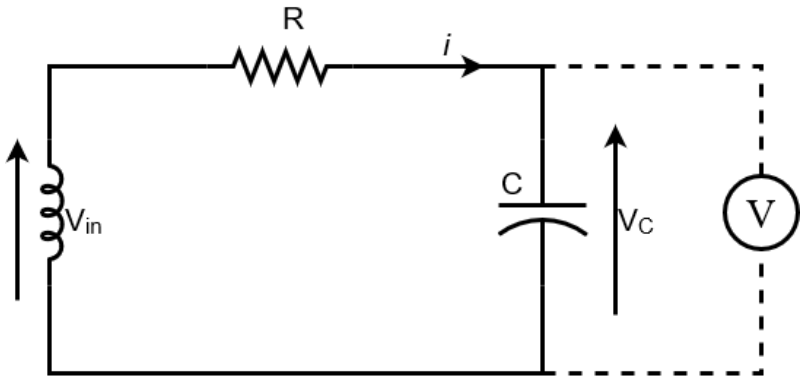

Figure 5.1: An RC integrator circuit for flux measurement

5.4 Search coil magnetometer

A search coil is a wire wounded around a magnetic material to measure the change in flux. It works according to Faraday's law of induction. The changing magnetic flux through the turns of the coil induces the voltage in the coil. This voltage is given by:

$$e = -N\frac{d\Phi}{dt} \tag{5.3}$$

where N is the number of turns and $\frac{d\Phi}{dt}$ represents the changing magnetic flux in the coil. The " − " sign represents opposite direction between both entities. A search coil is illustrated in the Fig. 5.2

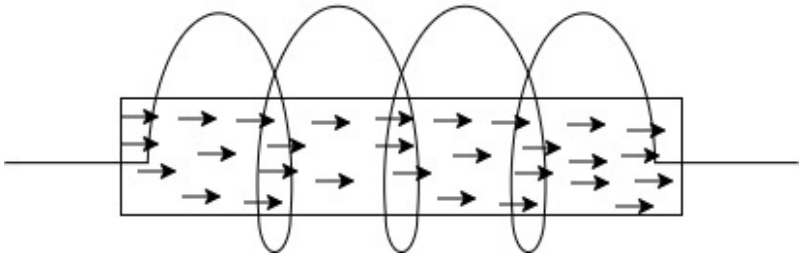

Figure 5.2: Search coil around magnetic flux carrying ferromagnetic material

In this thesis, the search coil of 10 turns was used for each measurement and excitation of bypasses. In this thesis, search coils were used for measurement of flux in both core types. Additionally these search coils were also used for the bypass excitation in hexa-core. The number of search coils used for different measurements in hexa-core and Evans core are given below:

1. List of different measurements for Hexa-core:
   - one search coil each, for the excitation of six bypasses.
   - one search coil each, for flux measurement in six bypasses.
   - one search coil each, for flux measurement in all the three windings.

2. List of different measurements for Evans core:
   - one search coil each, for the measurement of flux in A1 and A2
   - one search coil each, for flux measurement in bypass between A1 and A2.

5.5 Reference measurements for Evans and Hexa-core

Reference measurements were taken for both transformer core types, hexa-core and Evans-core. The reference measurement for the hexa-core transformer without bypasses was extracted from the previous work on this transformer and is presented in table below. In order to measure the loss reduction by introducing bypasses, a reference measurement or no-load measurement setup was developed. The transformer was connected in delta configuration and was excited through a 3-phase auto transformer. A 3 phase digital power analyzer was used to measure the phase voltages, phase currents and power losses in these windings. Transformer was connected to the current transformer and potential transformer of the power analyzer in a 3 phase 3 wire configuration. This configuration is also known as two Watt-meter method and is illustrated in the Fig. 5.3.

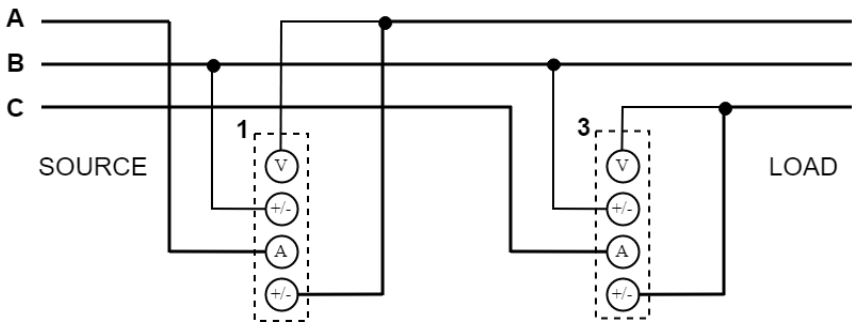

Figure 5.3: Two Watt-meter method

For the Evans core, a similar setup was established and is shown in Fig.5.4. In this method, one Watt-meter measures the instantaneous power in phase A and the other Watt-meter measures the instantaneous power in phase C and gives 3-phase average power for the connected load.

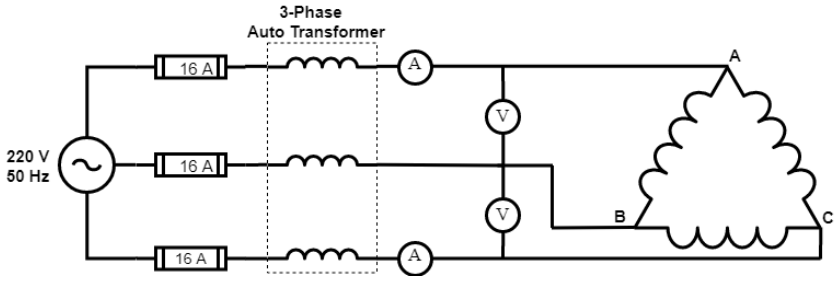

Figure 5.4: Measurement setup for both transformers

5.6 Bypass excitation

For bypass excitation a power electronics base active core strategy was developed which is discussed in detail in the forthcoming chapter. The bypass was wound with a coil and this coil was provided with a DC excitation source. The magnetic field strength because of auxiliary flux in the bypass can be calculated using the transformer formula:

$$V = \sqrt{2}\pi f N A B_{max} \tag{5.4}$$

Since the excitation coil is essentially an inductor wound around the bypass which in this particular case behaves as the core for such inductor. When this inductor is fed with a square wave from the converter, it behaves as a filter and the resultant flux is a sinusoidal with a fundamental frequency of 50 Hz.

For this application, frequency is 50 Hz whereas area for bypass is given to be 30% of the total cross section area of the core leg, number of turns for the auxiliary windings on bypass was selected to be 10 turns. With these values the required DC value for a particular magnetic field strength can be calculated.

6

Flux Control Strategy

This chapter introduces the strategies utilized in controlling the flux in the transformer core. As described in previous chapters a strategy comprising of introducing magnetic bypasses in the transformer can result in the reduction of excitation current hence results in reduction of excitation losses. Since it was established previously that Grain oriented bypasses have better performance as compared to Non-grain oriented bypasses, therefore Grain oriented bypasses are used in this thesis.

6.1 Power Electronics Based Active Core

As shown in the Fig. 6.1 the shape of flux in the winding is sinusoidal and hence it follows a hysteresis curve, where magnetic domains are aligned in both of the cycles. So the aim was to assist in this change in domain alignment and as a result excitation current from the supply can be reduced decreasing no-load losses.

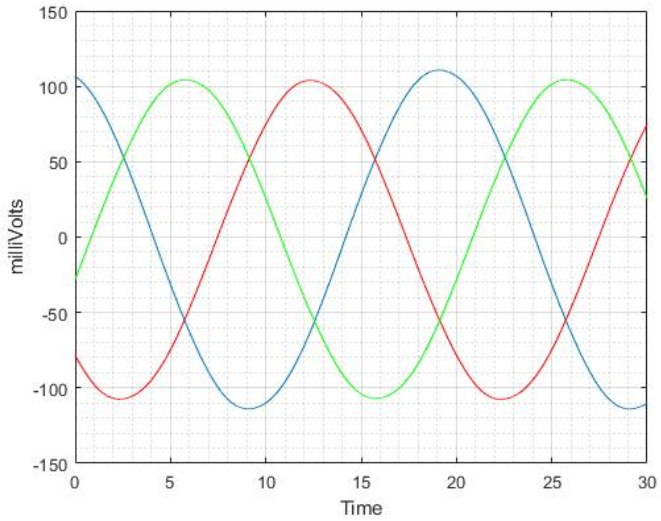

Figure 6.1: Flux in 3-phases

To influence the shape of flux in the bypass a power supply based on the feedback of main flux in the winding was designed. The main components of this power supply are described in the following sections. Fig. 6.2 shows a schematic diagram of the power electronics based power supply.

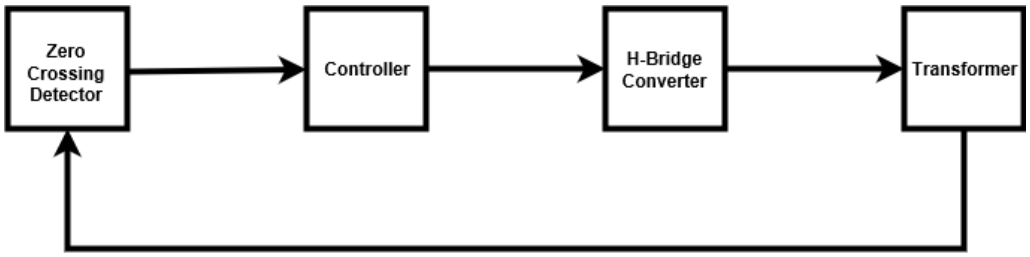

Figure 6.2: Schematics for active core flux control

6.1.1 Zero Crossing Detector

Since the bypasses are to be excited in synchronization with the point of zero crossing of the flux therefore a feedback is required. This feedback can either be taken from the flux in main winding or it can be taken from the flux in bypasses. But due to physical as well as practical limits the feedback was not taken from the flux in the bypasses.

An LM741 operational amplifier was implemented as a comparator so that a positive pulse was triggered as the flux in the main winding crossed the zero crossing before increasing to a positive value and zero pulse was triggered when the flux in the main winding crossed zero before decreasing to a negative value. The input to this zero crossing detector is taken from the output of search coil. The output waveform of such a zero crossing detector is given in the Fig. 6.3.

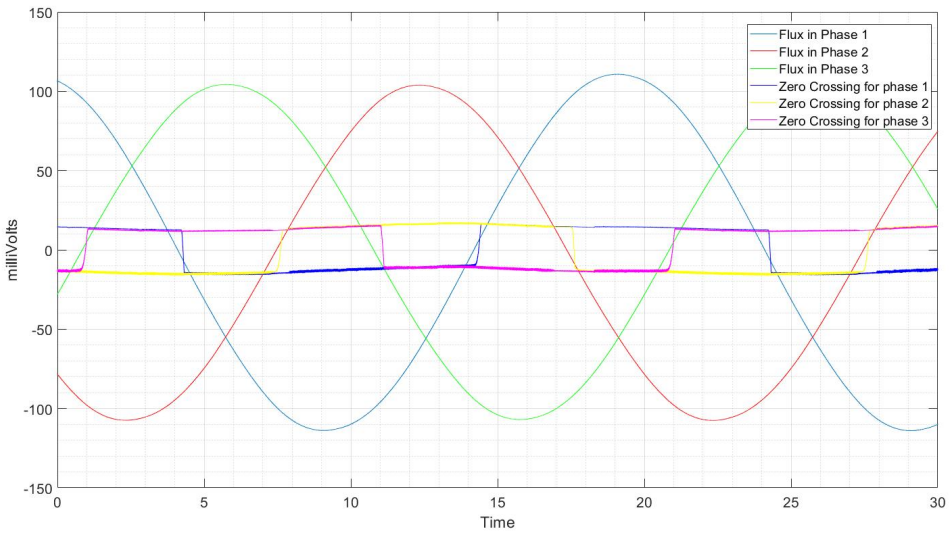

Figure 6.3: Waveform for zero crossing detector

6.1.2 Controller

As previously discussed, flux in the main winding is chosen as reference for zero crossing feedback, therefore a mathematical estimation for zero crossing in the bypass was implemented in a controller. From the previous work on the hexa-core and bypasses, it is established that the phase difference between flux in the bypass and main winding is 90°. Since the aim was to provide assistance during the period where flux changes its direction, therefore the auxiliary excitation was provided 30° after the peak of flux in the bypass. Based on frequency of 50 Hz that translates into 1.67 ms. So a delay of 1.67 ms was provided from the peak of the flux in the bypass as shown in Fig, 6.4.
Fig. 6.4 illustrates the working waveform of this power electronics based active core for one phase. The two sinusoidal waveforms represent the flux in main winding (core-leg A) and the respective bypass a. Further a square pulse is triggered by the controller at the zero crossing of the flux in main winding (green wave) and a gate excitation pulse for Mosfet in H-bridge is triggered after a numerical delay to synchronize with the bypass(purple wave).

In the waveform the position for excitation of one such bypass is given. Also one thing to be noticed here is that since there are 6 bypasses so 6 such converters were developed, one for each bypass. Since the bypass are constructed in a symmetrical form therefore two such symmetrical bypasses on the either side of transformer will have same zero crossing for flux but in opposite direction.

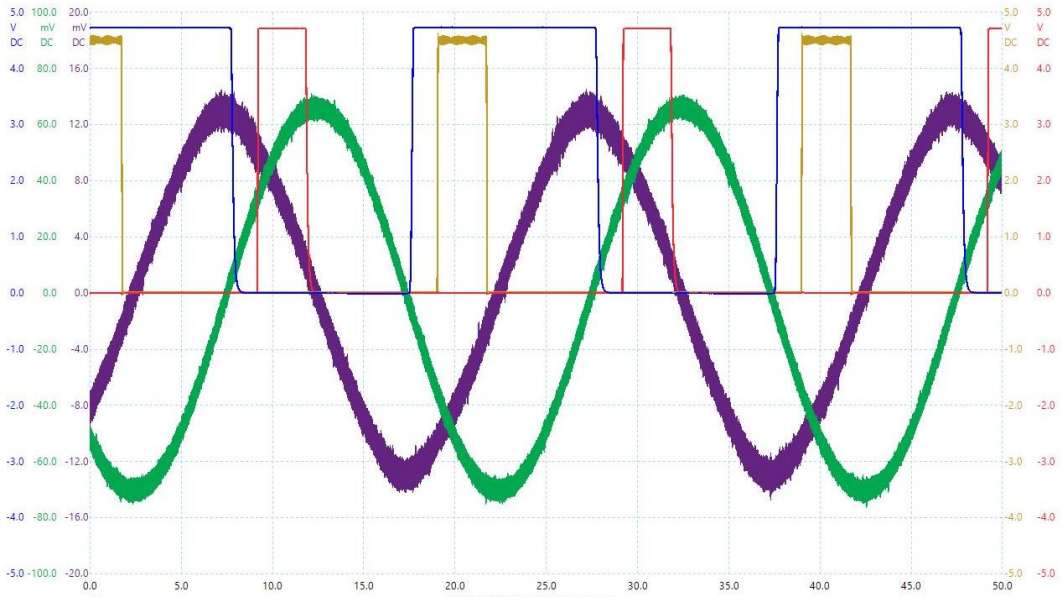

Figure 6.4: Excitation scheme for one bypass

Further to evaluate optimum point at which the bypasses could be excited the width of this pulse was also set to variable which can be tuned in controller.
The outputs from the zero crossing detectors for 3 main windings provide input to the controller and based on the calculations above outputs are provided to bridge

converter which can excite the bypasses through a DC source on during the time calculated.

6.1.3 H-bridge Converter

A complimentary pair H-bridge converter was developed to excite the bypasses. The $IRF2804$ n-channel Mosfets and $HA08p06$ p-channel Mosfets were used. The outputs of controller turn on and turn off Mosfets which in turn limits the operating voltage range for the converter, but it simplifies the circuitry in comparison with a dedicated gate drive circuitry. Fig. 6.5 shows the schematic for the H-bridge topology for controlling flux in one bypass.

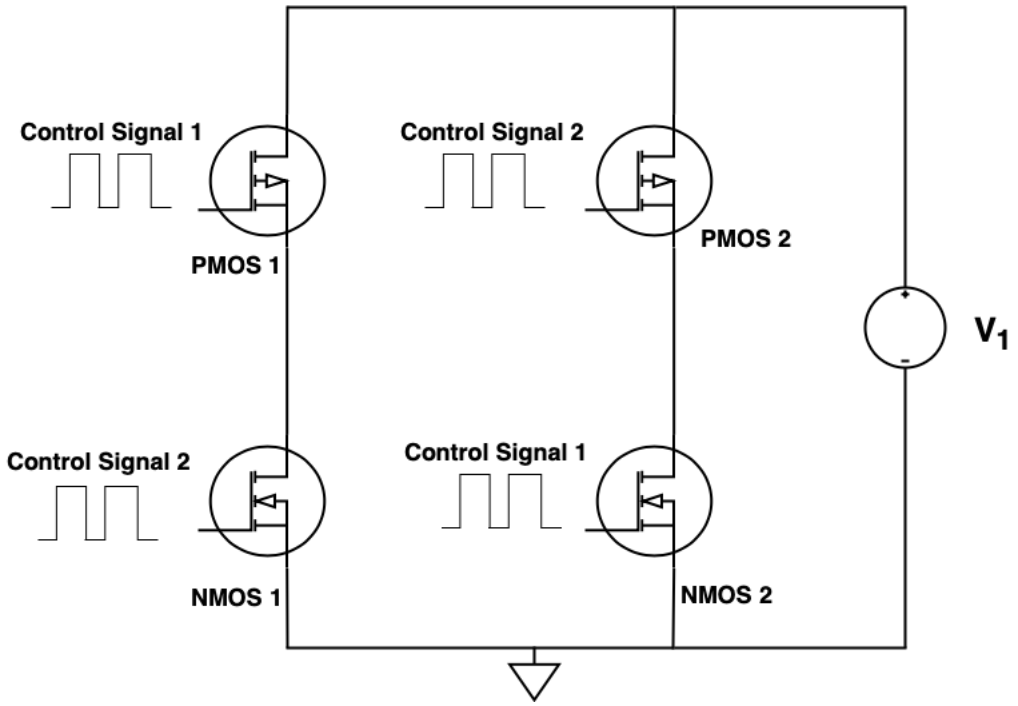

Figure 6.5: H-Bridge schematic for single bypass

The output of this converter is fed into a ten turn coil wound around the bypass producing magnetic field in the coil. The direction of this magnetic field is dependant on the voltage and magnitude of magnetic field is determined by the number of turns and magnitude of voltage. Given by the following equation:

$$V = \sqrt{2}\pi f N A B_{max} \tag{6.1}$$

So for current setup magnetic field of $1T$ is achieved by a voltage supply of 6 volts. This is also to be mentioned that this $1T$ field is superimposed on already existing field in the bypass. Since the coil wound around the bypass has a very small resistance therefore a current limiting resistance is also installed at the output of the current to limit the current which results an addition loss of 0.17 W. Six H-bridge circuits were used in in order to control the flux in all three limbs.

7
Results

In this chapter the results measured from various operating conditions of power electronics core are presented. Further the performance of Evans core and impact of magnetic bypasses on such a core is also evaluated.

This is to be noted that a transformer is usually operated between magnetic field strength which is lower then the saturation point which is around 1.9 T. Therefore an operating range of 1.2 T to 2.0 T is selected to evaluate the response of the developed prototypes.

In results the effect on two important quantities is evaluated. Firstly the no-load power loss, which are basically the excitation losses and secondly the loss angle alpha. The loss angle, alpha is the angle between A2 and the leg as described in the previous chapters. The usual value for this loss angle with grain oriented bypass was previously established to be 27° in case of hexa-core. Therefore figures illustrating comparison between previously established loss angle and impact of bypass excitation are presented in this chapter.

The value for loss angle in case of an Evans Core is also determined graphically which is presented in the later sections. The emphasis on role of this loss angle in performance of transformer is described in previous chapters.

7.1 Loss reduction with Active Core

In this section the influence of active core on the excitation losses in transformer is presented. A step by step approach was taken in order to evaluate the outcomes, and the outcomes are presented in the following sections.

7.1.1 Influence of each bypass

Since it is very important to know, how much flux in the transformer can be influenced with excitation of each bypass. Therefore bypass excitation was added progressively and the change in loss angle and excitation loss was recorded. The operating value of excitation level was selected to be 1.5 T in the main core which gives an operating voltage of 18.5 V. The input DC excitation voltage was at 6 V so that the auxiliary exciting level in the bypass is around 1 T. Tab. 7.1 shows the

loss in power with increase in the number of bypasses being energized.

Excitation of successive bypasses	
No. of bypasses excited	Power Loss [**W**]
Zero/No bypass	7.458
One	7.409
Two	7.362
Three	7.309
Four	7.261
Five	7.213
Six	7.161

Table 7.1: Effect of excitation on bypasses at 1.5 T in the core leg

The Fig. 7.1 below shows the change in the loss angle with excitation of no bypasses and 6 bypasses respectively.

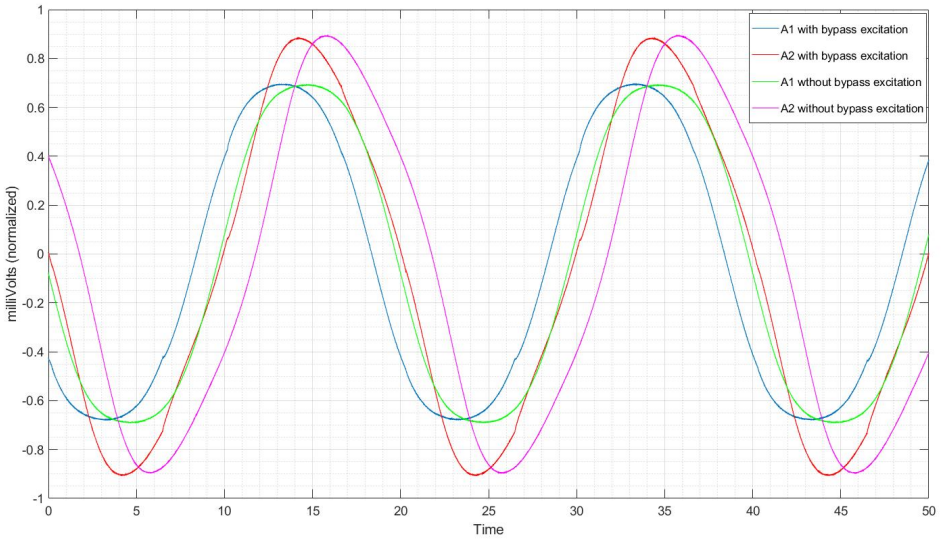

Figure 7.1: Decrease in loss angle with bypass excitation

7.1.2 Influence of flux in main core

As previously described the operating range considered for the test transformer is between 1.2 T to 2.0 T therefore the next logical evaluation is evaluating the behavior of losses with variation in the excitation level in the main core. As an initial assessment the reference measurement for the losses are done and are presented in the Tab. 7.2. These reference values are also verified against the previous work done on the core and are found in coherence with the previously established values.
Next all six bypasses were excited with power electronics circuitry to provide auxiliary magnetic field strength of 1 T in the bypasses and the resulting losses in

Power loss in bypass at different feeding voltages		
Voltage [**V**]	Excitation [**T**]	Power Loss [**W**]
12.66	1.00	1.1
14.00	1.10	3.056
16.00	1.26	4.145
18.00	1.42	6.531
18.98	1.50	7.342
20.00	1.58	8.483
21.52	1.70	9.894
22.00	1.74	11.989
24.00	1.86	16.784
25.00	1.90	24.323
25.30	2.00	52.457

Table 7.2: Variation of power loss with excitation level between 1.2 T and 2.0 T

Watts are presented in the table below. It should be noted that with magnetic field strength in bypasses fixed the input power to provide auxiliary magnetic field in the bypasses is also constant. Further from the table a decrease in losses can be seen, however the behaviour of core is nearly similar to that without auxiliary magnetic field in the bypasses i.e it reaches saturation nearly to the 1.90 T.

Power loss in bypass at different feeding voltages		
Voltage [**V**]	Excitation [**T**]	Power Loss [**W**]
12.66	1.00	1.075
14.00	1.10	2.921
16.00	1.26	4.396
18.00	1.42	6.248
21.00	1.70	9.445
24.00	1.86	16.213
25.30	2.00	50.875

Table 7.3: Variation of power loss with excitation level between 1.2 and 2.0 T

As previously discussed a tendency of core to reach saturation near 1.75 T can be seen from the experimental results, however for general behaviour 1D interpolated curve is shown in the figure below.
From these interpolated plots it can be seen that with bypass excitation, at same magnetic field strength lower excitation losses are incurred in the main core. For instance at 1.7 T the loss for core without excitation is nearly 10.02 W where as with bypass excitation it is nearly 9.4 W. It is to be noted that in such transformers the region between 1.2 T to 1.9 T is of significant importance to us since transformer is mostly operated between this region.

As previously discussed, at 1.7 T a difference in power losses between two arrangements is nearly 0.467 W, which translates into 4.6 %. Fig.7.4 represents the loss reduction in percentage over the range of 1.20 T to 2.00 T.

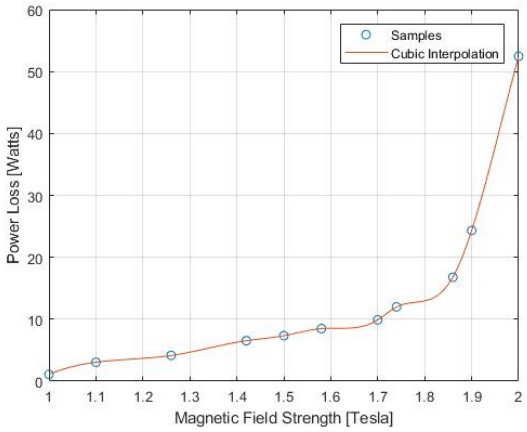

Figure 7.2: Reference loss curve

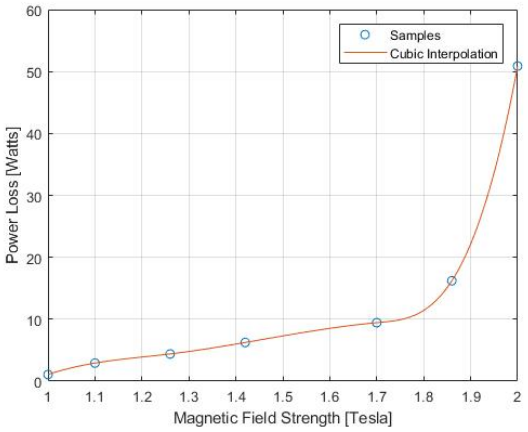

Figure 7.3: Loss curve with bypass excitation

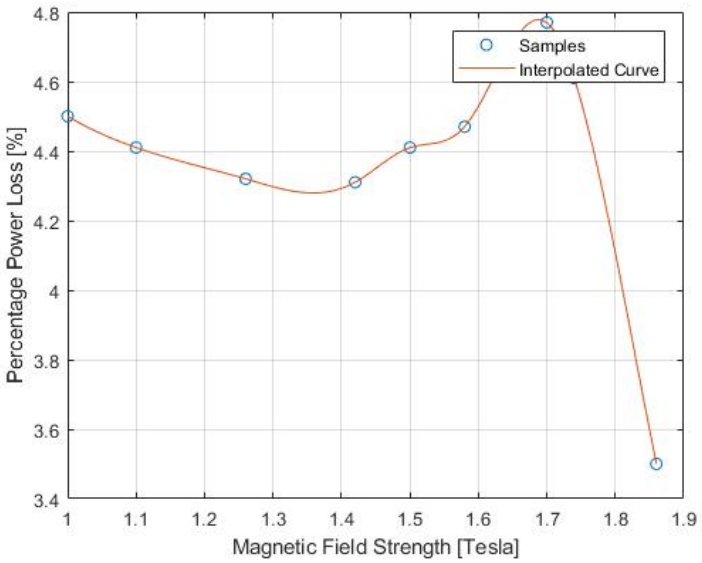

Figure 7.4: Percentage loss reduction

From the Fig. 7.4 it can be seen that the impact of bypass excitation achieves a peak value of 4.48 % reduction in power loss nearly at 1.75 T. However it should also be noted that the decrease in power loss decrease significantly after saturation due to increasing copper losses.

7.1.3 Influence of DC excitation

Further the voltage for excitation of bypasses is varied from 6 volts to 12 volts keeping the magnetic excitation in the main core at 1.5 T and the results are presented in the Tab. 7.4.
This increase in voltage corresponds to an increase in magnetic excitation from 1.2 T to 1.7 T. This increase in auxiliary excitation is also complemented by the increase

Influence of DC excitation on losses	
DC Voltage [**V**]	Power Loss [**W**]
6.00	7.161
8.00	7.088
10.00	7.225
12.00	7.230

Table 7.4: Variation of power loss with DC voltage between 6V and 12V

in input DC power from 0.456 to 1.3 W where as from the Tab. 7.4 the maximum difference achieved in excitation power loss is as low as 0.069 W. While analyzing and deducing conclusion this factor should also be taken in consideration. These results give us a good idea regarding discrete operating points but to obtain a general behaviour of core to this type of so called auxiliary excitation an interpolated figure of these discrete points is presented in Fig. 7.5.

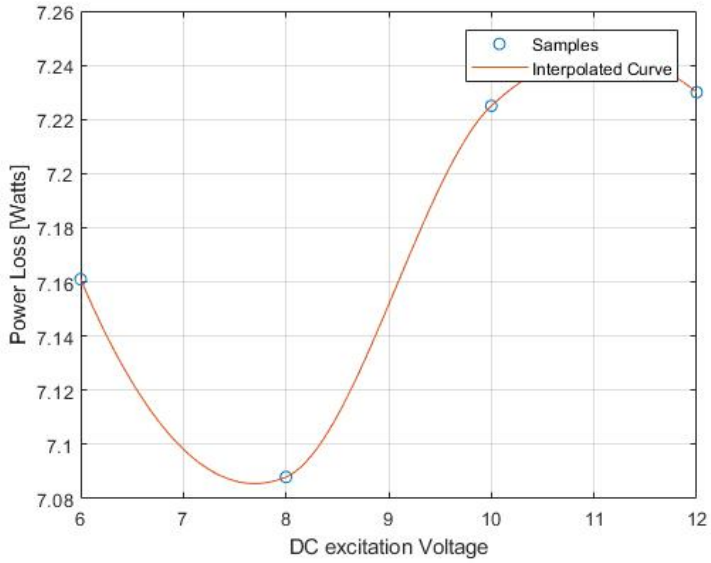

Figure 7.5: Variation in losses with change in DC excitation

From Fig. 7.5 it can be seen that there is a tendency of material to further reduce losses with the increase in voltage and then the losses in main core sharply increase with further increasing the auxiliary excitation voltage. Here it is important to consider that all other perimeters for the transformer such as the main excitation (excitation level in core legs), the wire resistance, the current through the main windings, etc are same and yet there is an increase in losses from the set-point value which was previously established to be 7.16 W.

This sharp increase can be attributed to the fact that with increase in the auxiliary excitation, the bypasses are driven into saturation region earlier than the main core hence the control on the flux domains is lost, but this requires further investigation to be explained. However the decrease in power loss is on expense of input DC

power which should also be paid attention to while considering such prototype.

7.1.4 Influence of pulse width

Next the width of the firing pulse shown in Fig. 6.4 was varied keeping the excitation value at 6 V and the results are presented in the Tab. 7.5.

Influence of pulse width on losses	
Pulse Width [**ms**]	Power Loss [**W**]
2.00	7.368
4.00	7.165
6.00	7.285
8.00	7.452

Table 7.5: Variation of power loss with pulse width from 2 ms to 8 ms

From Tab. 7.5 it can be seen that pulse width of such auxiliary excitation is also critical. With the increase in pulse width essentially there is an increase in the voltage hence an increase in the excitation level. Further with the increase in time delay as it can be seen in Fig. 6.4 the pulse overlaps with the region where magnetic domains have in fact opposite direction to that of the pulse hence further increasing the losses. As can also be seen from the Fig.7.6.

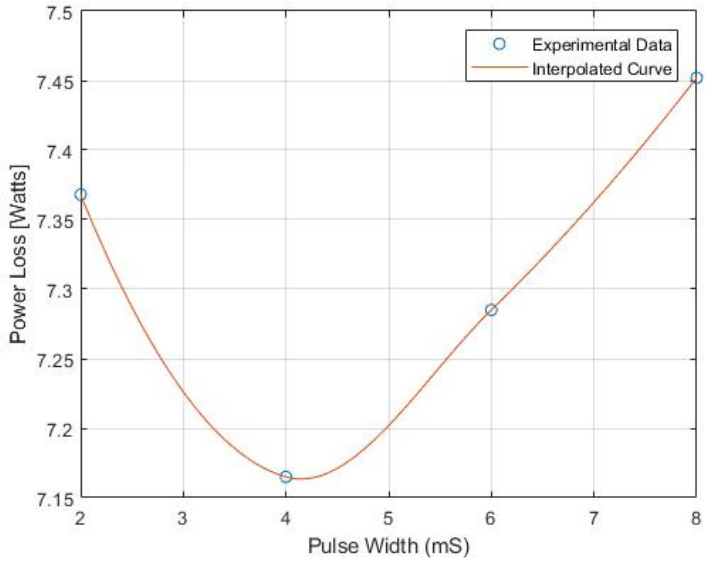

Figure 7.6: Variation in losses with change in pulse width

7.2 Evans Core Evaluation

In this section the results with tests performed on the Evans core are presented. Since both Evans core and hexa-core are wound cores therefore a similarity in be-

haviour of magnetic circuit for both of them can be expected. However since in Evans core the outer core ring is not of the similar length as of two inner rings therefore some asymmetry can be expected.
Initially the core was excited without any bypasses or supplementary methods to reduce losses and later with bypasses. Further it is to be noted that the bypass were installed on the one side of the transformer core and the presented results illustrate the influence of the bypasses on one side.

7.2.1 Reference Measurement

Tab. 7.6 presents results for Evans core without any bypass arrangement attached to it.As previously established that the range between 1.2 T and 2.2 T are of interest to us therefore the transformer was tested between this range. From Tab. 7.6 it

Power loss in bypass at different feeding voltages		
Voltage [**V**]	Excitation [**T**]	Power Loss [**W**]
10.52	0.8503	1.72
12.19	0.9331	2.29
14.01	1.0725	2.94
16.23	1.2424	3.95
18.09	1.3848	4.93
20.31	1.5547	6.42
22.17	1.6971	8.27
24.03	1.8395	11.3
26.02	1.9918	18.9
28.02	2.1449	55.3

Table 7.6: Variation of power loss with excitation level between 1.2 and 2.0 T

can be seen that with the increase in magnetic field there is an increase in losses however these sharply increase near 1.9 T and keeps on increasing exponentially. After saturation, the losses in the core(iron losses) do not increase significantly but the losses in the copper are increasing exponentially. Since both losses are being measured and at saturation the criteria to neglect copper losses is not valid anymore due to high currents, this results in very high losses in the transformer.

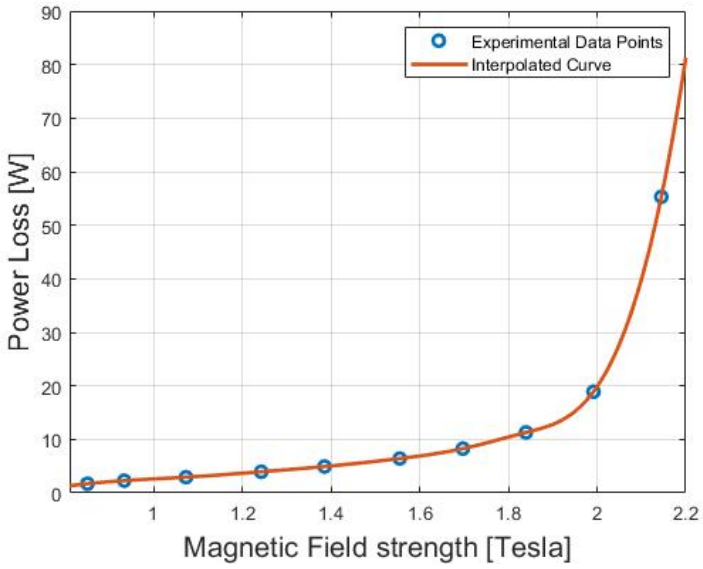

Figure 7.7: Reference loss curve for Evans core

Further to complement the information from the table these experimentally obtained data points are presented in 1D interpolated curve in Fig. 7.7. Here again from this curve it can be seen that the losses keeps on increasing exponentially once the core has reached the saturation region.

Next important perimeter to be evaluated is the flux in core. The presented results are the flux in core ring A_1 and A_2, which constitutes the inner two rings of the transformer core. These flux are taken with reference to core in the center leg **A**. Further these flux are plotted for four different magnetic field strength values to have an idea of flux shape at these different values.

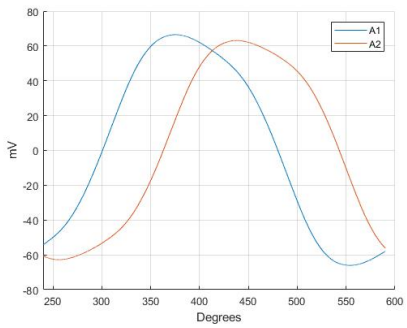

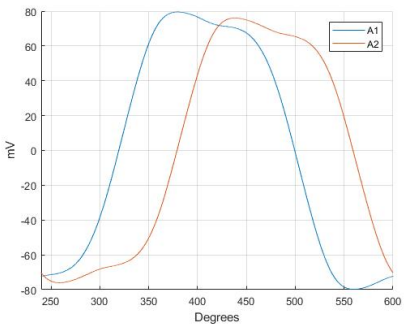

Figure 7.8: Flux in A1 and A2 at 1.2 T **Figure 7.9:** Flux in A1 and A2 at 1.5 T

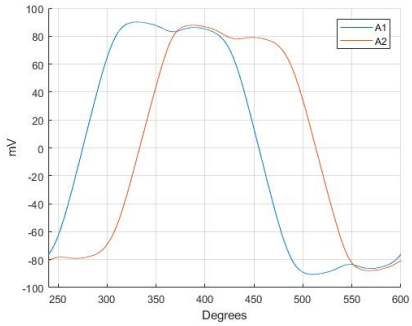

Figure 7.10: Flux in A1 and A2 at 1.8 T

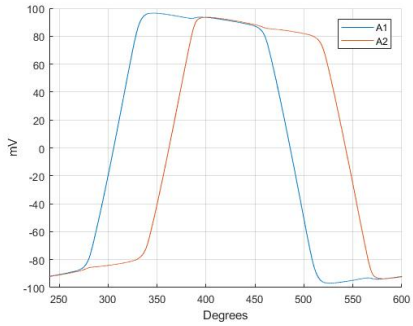

Figure 7.11: Flux in A1 and A2 at 2.1 T

From these figure firstly it can be established that the angle between A_1 and A_2 is 57.47° which gives a loss angle α of 27.91° at 1.5 T. Since the core rings A_1 and A_2 have a flux that should be 15% (without bypass) higher than (summarized) in the leg hence they are faster into saturation than the measured induction in the leg. e.g having 1.8 T in the leg results in $1.8\ T \times 1.15 = 1.98\ T$ in the core rings. It has been observed that from Fig. 7.8 to Fig. 7.11, the core has reached its saturation region and that gives the flat curve (and a more rectangular form, with higher derivative and flat top).

7.2.2 Evaluation of different bypass strategies

As described in Section 3.2 different bypass strategies for reduction of excitation losses were tested and the results are presented in the consequent sections.

7.2.2.1 Bypass EGO-1

First bypass to be evaluated is EGO-1. The Tab. 7.7 shows results from measured losses for such arrangement at different magnetic field strengths. Furthermore in the presented results, the bypass area is 20% of the cross section area of the core leg.

Power loss in bypass at different feeding voltages		
Voltage [**V**]	Excitation [**T**]	Power Loss [**W**]
10.02	0.7670	1.48
12.36	0.9462	2.083
13.95	1.0679	2.684
16.46	1.2600	3.501
18.43	1.4108	4.521
20.49	1.5685	5.500
22.28	1.7055	7.336
24.45	1.8716	10.947
26.69	2.0431	23.896
27.89	2.1350	47.971

Table 7.7: Variation of power loss with excitation level between 1.2 and 2.0 T

To predict behaviour of the bypass an interpolated loss curve with the reference curve previously established are presented in the Fig. 7.12. Here it can be seen that 11% loss reduction can be achieved at 1.5 T.

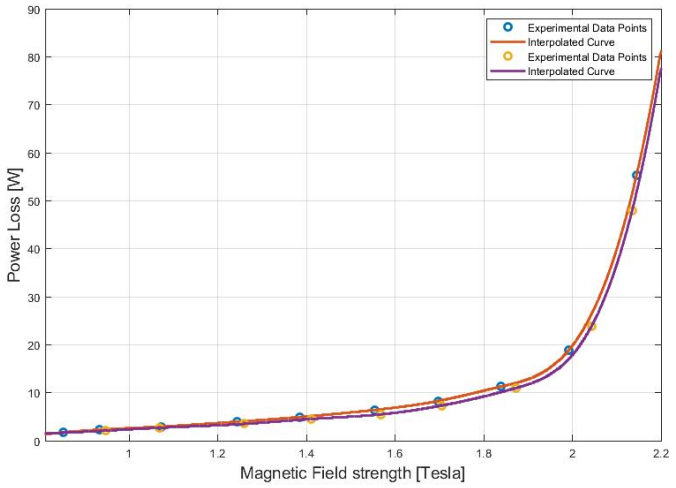

Figure 7.12: Effect of EGO-1 on no-load losses

Next the flux distribution in the core and bypass are evaluated and the results are presented in the figures below. The measurements presented, follow the same reference as previously discussed i.e flux in inner core rings A_1 and A_2, flux in main leg A. However these figures, from Fig. 7.13 to Fig. 7.16, also incorporate the flux in bypass referred to as **a**.

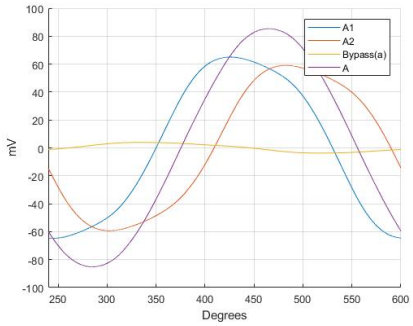

Figure 7.13: Flux distribution in transformer core at 1.2 T

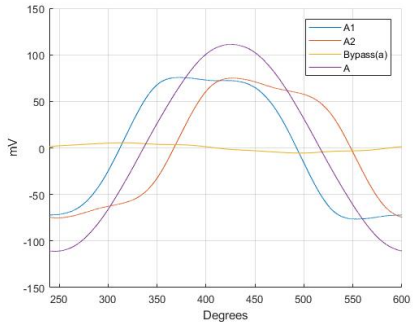

Figure 7.14: Flux distribution in transformer core at 1.5 T

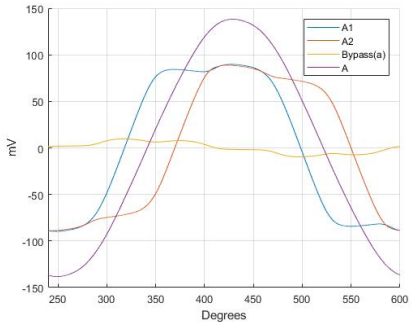

Figure 7.15: Flux distribution in transformer core at 1.8 T

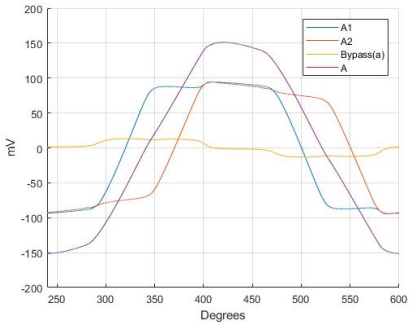

Figure 7.16: Flux distribution in transformer core at 2.1T

By analysing above figures, from Fig. 7.13 to Fig. 7.16, it can be established that A_1 and A_2 are 56.8° apart at 1.5 T which translates to a loss angle α of 27.1°. Further a general idea of flux in the core can also be deduced from these figures. An important perimeter to be noted in these figures is the flux in bypass **a**. It can be seen that the shape of **a** keeps on distorting as the magnetization is increased. Further at 1.5 T a total of 9.8 % of the total flux in the leg passes through the bypass.

7.2.2.2 Bypass EGO-2

Next bypass evaluated is EGO-2, as shown in Fig. 3.7. The Tab. 7.8 presents results from measured losses for such arrangements at different magnetic field strengths. Furthermore in the presented results, the bypass area is 30% of the cross section area of the core leg.

Further to predict behaviour of the bypass over the range of magnetic field strength, an interpolated curves of experimentally obtained values with bypass and the reference values are presented in Fig. 7.17. Here it can be seen that at 1.5 T, 15 % can be achieved using this bypass strategy.

Power loss in bypass at different feeding voltages		
Voltage [**V**]	Excitation [**T**]	Power Loss [**W**]
10.16	0.7777	1.368
12.11	0.9270	1.683
14.16	1.0839	2.533
15.98	1.2233	3.221
18.91	1.4476	3.808
20.03	1.5333	4.471
22.50	1.7224	6.477
24.63	1.8854	8.330
26.84	2.0546	20.655
28.02	2.1449	42.670
29.06	2.2245	75.055

Table 7.8: Variation of power loss with excitation flux between 1.2 and 2.0 T

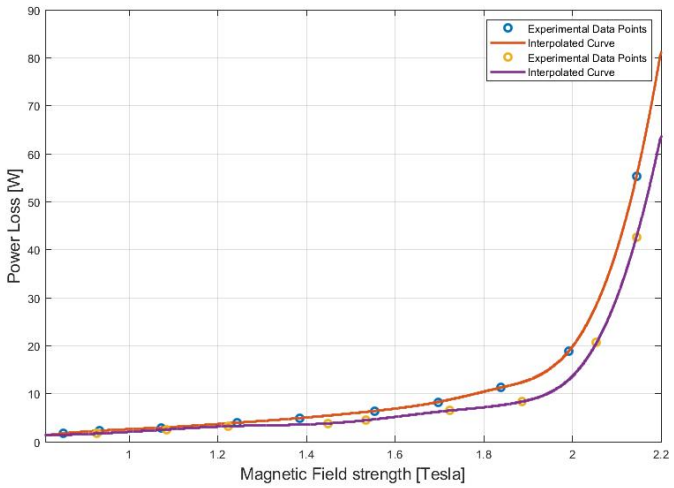

Figure 7.17: Loss curve with EGO-2

Further the flux distribution in the core and bypass is shown in the figures below. The measurements shown in the figure follow the same reference as of the previous figures.

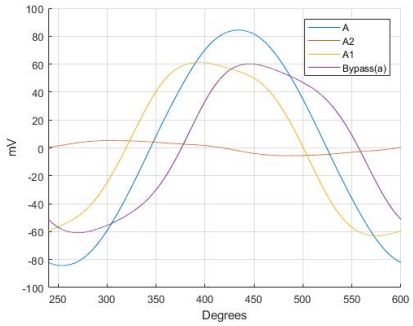

Figure 7.18: Flux distribution in transformer core at 1.2 T

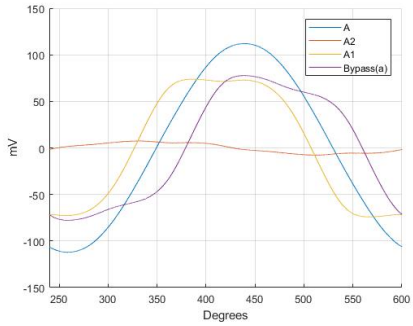

Figure 7.19: Flux distribution in transformer core at 1.5 T

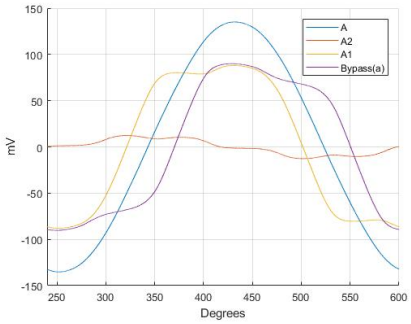

Figure 7.20: Flux distribution in transformer core 1.8 T

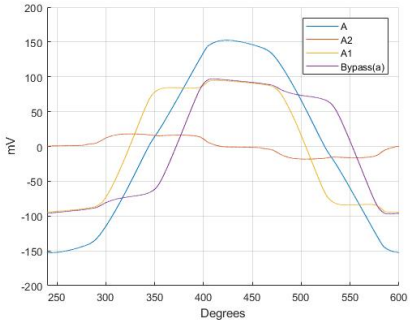

Figure 7.21: Flux distribution in transformer core at 2.1T

From these figures it can be seen that A_1 and A_2 are 55.4° apart at 1.5 T which translates to a loss angle α of 26.8°. In this type of bypass a total of 13.57 % flux passes through the bypass at 1.5 T.

7.2.2.3 Bypass EGO-3

Bypass EGO-3 as shown in figure 3.8 was evaluated and the results are presented in Tab. 7.9. Furthermore in the presented results, the bypass areas are 25% of the cross section area of the core leg.

Fig. 7.22 presents interpolated curves for reference measurement and measurement with bypasses to show a general behaviour of such a transformer for different magnetic strength behaviour. Here it can be seen that a total of 5 % at 1.5 T reduction in losses can be achieved.

Power loss in bypass at different feeding voltages		
Voltage [**V**]	Excitation [**T**]	Power Loss [**W**]
10.19	0.7800	1.529
12.37	0.9469	2.325
14.56	1.1146	2.954
16.19	1.2393	3.686
18.58	1.4223	4.835
20.32	1.5555	6.061
22.76	1.7423	8.483
24.07	1.8426	10.640
24.96	1.9107	13.490
26.09	1.9972	18.145
28.51	2.1824	64.980
28.89	2.2115	75.810

Table 7.9: Variation of power loss with excitation flux between 1.2 and 2.0 T

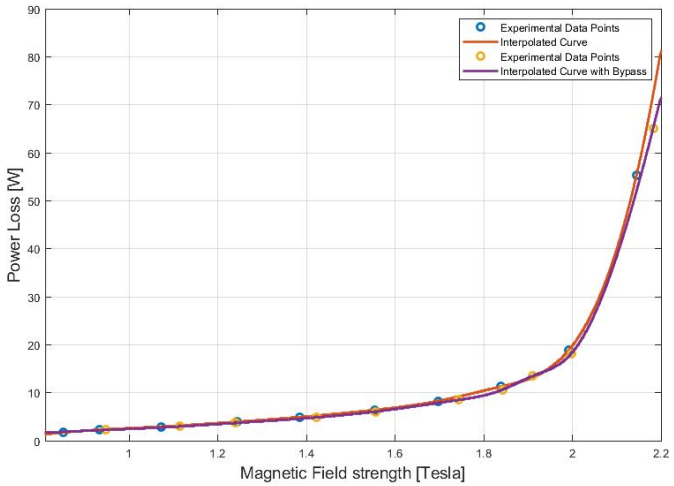

Figure 7.22: Loss curve with EGO-3

The flux distribution for such an arrangement are presented in the figures below. From these figures it can be deduced that A_1 and A_2 are 56.23° apart from each other in this case. For which exists a loss angle α of 27.12°. Bypass constitutes 11.23 % of the total flux in the core.

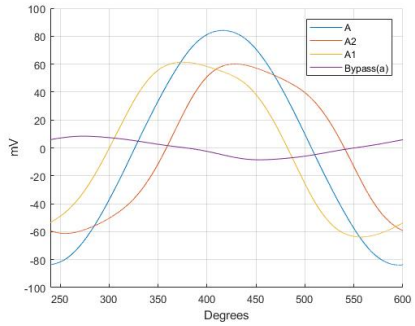

Figure 7.23: Flux distribution in transformer core at 1.2 T

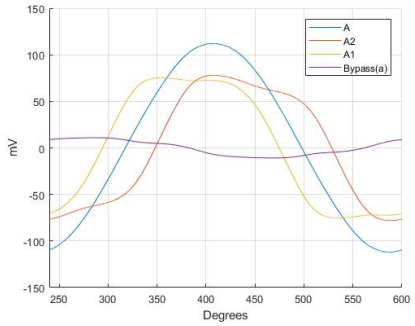

Figure 7.24: Flux distribution in transformer core at 1.5 T

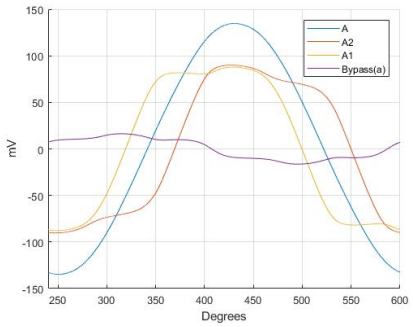

Figure 7.25: Flux distribution in transformer core 1.8 T

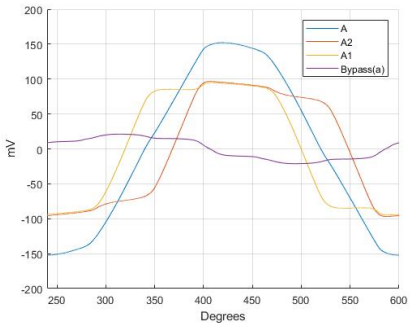

Figure 7.26: Flux distribution in transformer core at 2.1T

8

Analysis

In this chapter, results from the effect of different bypass configuration on the reduction of no load losses in transformer will be discussed and analyzed. further the effect of bypass excitation on loss reduction in hexa core transformer will be analyzed. Finally a comparison of different bypasses will be done and the most effective bypass configuration will be chosen.

8.1 Hexa-core transformer

As from previous studies done on the transformer core the optimum choice for type of bypass arrangement and the weight of such a bypass was suggested. In this project methods to further decrease losses using alternative methods were tested. It is to be noted that the decrease in losses discussed in this report are superimposed on the decrease previously achieved.

8.1.1 Reduction of losses with bypass excitation

An inherent property of a magnetic material is the tendency of avoiding change in the shape of magnetic domains in the material. This translates into a hysteresis loop for the material as discussed in section 2.3.1.2. With the implementation of power electronics circuitry it can be seen that a significant amount of load on the primary excitation can be reduced. As from Fig. 7.25 it can be seen that when flux in the main core is around 1.8 T the bypasses tend to have a flatter top as compared to low flux values. Hence if we are successfully able to step ahead of hysteresis loop and re-align the magnetic domains in the materials the losses can be reduced.

Further while being ahead of the hysteresis loop it should be noted that at high flux values the core can be saturated hence loosing the impact of auxiliary excitation. From Fig. 7.6, it can be seen that the losses tend to increase if increase the duration of excitation which can be credited to the fact that after the flux crosses the zero crossing it changes its polarity and opposing the flux at this instant increases the losses in the core.
The correct phase of excitation can be emphasized from the Fig.7.6. It can be seen that loses tend to increase if we further delay the excitation which is also again attributed to the fact that the instant of excitation should not coincide with re-aligning of flux in opposite domain. It is also to be noted that if the excitation

starts earlier in phase then the input power is increased without providing much assistance.
By and large from aforementioned observations it can be deduced that by introduction of such active core a reduction in losses can be observed, however this decrease in losses is on expense of input DC power. Therefore while designing such an equipment it is important to keep the input power under consideration as well.

8.2 Evans core transformer

As previously described Evans core and hexa-core are wound cores, therefore a similar behaviour was expected which was further proved by the results. However from the geometries of both the transformers it can be seen that in case of hexa-core the three main core legs are 60° to each other. Therefore the distance between all three legs is same hence creating a symmetry. This symmetry in geometry results in a symmetry in the flux distribution in the core. However Evans core has a flat arrangement which results in one of the leg being closer than other. Hence the flux distribution in such case is not symmetrical. Furthermore it can be inferred that the turning angles are higher (up to 360° instead of maximum 120° due to flat arrangement (planar core) and that increases the reluctance in the bypass for Evans core.

8.2.1 Comparison of different bypass configuration

The table 8.1 shows the results form these bypasses and a comparison of different parameters. In this table, performance of all bypasses used are evaluated. The first bypass has the lowest added weight and it shares a total of 8.99 percent of total flux whereas the similar configuration used in EGO-2 with wider bypass and covering 35.2 percent cross-sectional area of the core does not make enough difference in the loss reduction while it shared more flux than the previous configuration. The third configuration having approximately equivalent weight to the EGO-1 shares the higher amount of flux than the others but does not decrease the losses at all. In this configuration most of the energy is utilized/destroyed in the bypass itself and it does not reduces the overall losses. From this table 8.1, it is seen that EGO-2 reduces the highest amount of losses but if one considers the amount of added iron, then it has the highest amount of iron to reduce the losses. It is a trade off between loss reduction verses the amount of added iron in the core.

Performance and comparison of different bypasses			
Type of Bypass	Weight of bypass added [g]	CSA [%] of core leg	Flux in bypass [%]
EGO-1	488	26.6	8.99
EGO-2	961	35.2	11.9
EGO-3	506	26.1	8.78

Table 8.1: Performance and evaluation of different bypasses

Fig.8.1 illustrates loss reduction at each value of magnetic excitation for all three bypasses. Here it can be seen that highest loss reduction achieved using EGO-2 bypass is ca. 15% around 1.7 T. The figure provides a decent analysis of the performance of each bypass in terms of loss reduction.

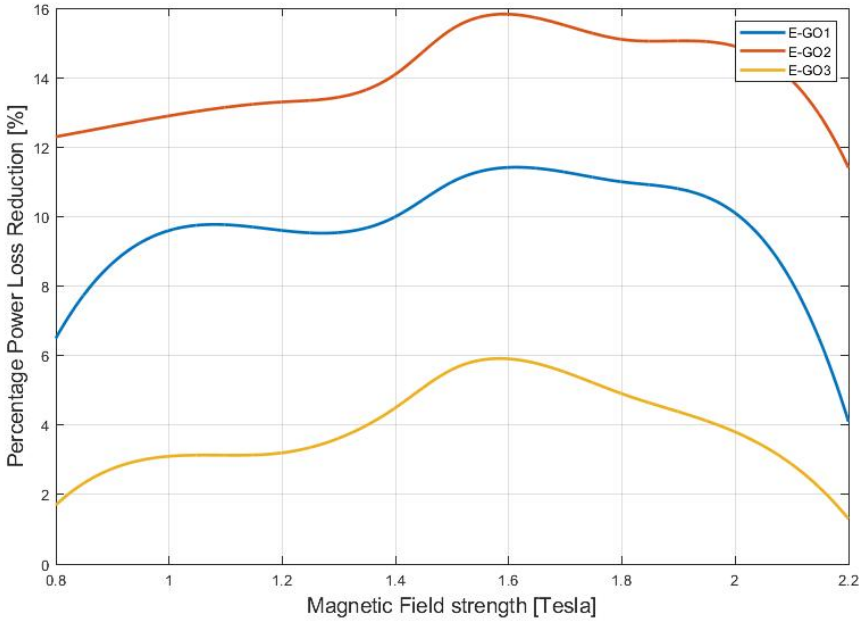

Figure 8.1: Percentage loss reduction with different bypasses

9
Conclusion

Previous work done on hexa-core transformer showed that no-load losses in a transformer can be reduced using bypass strategy. The bypass strategy implemented was aimed at creating new flux paths in the transformer core in order to reduce the no-load or excitation losses in a transformer.

Extending the previous work, this thesis was aimed at further reducing these losses to comply with the new EU Commission regulations. First, utilizing the existing work done on hexa-core, an auxiliary excitation scheme for the so called bypasses was developed using power electronics. This auxiliary excitation was made to synchronize with the flux in main windings on core leg. This synchronization targeted in aiding the dynamic alignment of magnetic domains in the core hence named *ActiveControl*. This implemented strategy reduced losses in the transformer further by ca. 4.5%.

Another type of wound core transformer known as Evans-core was tested for no-load losses using different bypass configuration. Being a wound core it somewhat showed similar behaviour to the hexa-core, this can be seen by the behaviour of flux in the core.

Further three different bypass strategies were implemented and tested for loss reduction in Evans-core. These bypasses effectively reduced losses depending on the arrangement and magnetic field strength in the transformer core. As previously mentioned such bypasses are implemented to provide alternate flux paths with in the wound core transformers, the bypass implemented were able to exploit this as can be seen by the percentage of flux that travels through the bypass.

Further the implemented bypasses were able to reduce losses depending on the arrangement of the bypass and the excitation field strength in the main core. At the end of this thesis, it was concluded that the bypass configuration EGO-2 for the Evans core exhibits the best results in reducing no-load losses.

10
Future works

Since requirement for transformer efficiency is a critical aspect in a sustainable power system, therefore there will always be room for improvement. Materials to be used, transformer size, affordability, reliability and electrical performance are some essential aspects of future transformer development.

This project was based upon the efficiency aspect of the transformer. The developed power electronics circuitry however performed as per aspirations and proved to be vital in terms of reducing no load losses, but an important perimeter is the input DC power. The designed power electronics was based on a square wave input converters. However it will be interesting to see the outcome if the converter outputs an SPWM (Sinusoidal Pulse Width Modulation).

The secondary voltage in hexa-core transformer includes number of harmonics. The method investigated in this report does not provide enough conclusion on the interaction of auxiliary flux with these harmonics. Here an SPWM which follows the main flux might be more influential to cause changes in the secondary voltage.

The bypass used for loss reduction in Evans core were used only one side of the transformer.So it will be interesting to see how these bypasses coupled with bypasses on the other side influence the losses. However in case of hexa-core transformer the loss reduction was doubled as a result of using bypass on both sides.

Further the developed power electronic prototype for hexa-core might be more complex in construction for Evans-core but it will be interesting to see how the electronics interact with the Evans core.

Bibliography

[1] European Environment Agency, "Overview of electricity production and use in Europe" 2018, Accessed Online on June 01, 2019, //www.eea.europa.eu/downloads/197d768aa294450eaa464d17b56c3dfc/1556552580/assessment-4.pdf

[2] Implementing EPA's Clean Power Plant," Reduce Losses in the Transmission and Distribution System" \http://www.4cleanair.org/sites/default/files/Documents/Chapter_10.pdf

[3] Effect of magnetic bypass on performance of hexa-core distribution transformer" \http://publications.lib.chalmers.se/records/fulltext/255810/255810.pdf

[4] Vladimir Lebedev, "Transformer Basics," 2007 Electrical Insulation Conference and Electrical Manufacturing Expo,Nashville,TN,USA, 2007, pp. 1-4. DOI:10.1109/EEIC.2007.4562642

[5] S. Lundmark, Y. V. Serdyuk, S. M. Gubanski and B. Larking, "Comparison between hexa- and conventional E-type core three-phase transformers," 2008 18th International Conference on Electrical Machines, Vilamoura, 2008, pp. 1-6. DOI: 10.1109/ICELMACH.2008.4799835

[6] B.A CALHOUN, "Ferromagnetic materials," 2016 Washington,DC,USA,pp. 1-4.

[7] A.Coombs, M.Lindenmo,D.Snell,D.power "Review the types,properties,advantages and latest developments in insulated coatings on non oriented electrical steels," 2001 Transactions on Magnetics, pp. 1-14. DOI:10.1109/20.914376

[8] Eddy current and hysterisis looses" Accessed Online on June 01, 2019, \http://thesis.com/papers/ICIEEE/K085093.pdf

[9] F. De Leon,A. Semlyen "A simple representation of dynamic hysteresis losses in power transformers," jan 1995 Transactions on Power Delivery, pp. 315-321. DOI:10.1109/61.368383

[10] G. Swift, T.S. Molinski, W. Lehn "A fundamental approach to transformer thermal modeling. I. Theory and equivalent circuit," april 2001 Transactions on Power Delivery, pp. 171-175. DOI:10.1109/61.915478

[11] Michael J. Thompson, Hank Miller,John Burger "AEP experience with protection of three delta/hex phase angle regulating transformers. 2007 Power Systems Conference: Advanced Metering, Protection, Control, Communication,

and Distributed Resources,Clemson, SC, USA " 13-16 march 2007, pp. 1-10. DOI:10.1109/PSAMP.2007.4740903

[12] Commission Regulation (EU) No 548/2014,

A

Appendix 1

SPECIFICATIONS

In terms of maximum core loss, AK Steel CARLITE Grain Oriented Electrical Steel specifications are determined at 1.5 T and 1.7 T at 50 Hz. Core loss grading is conducted using as-sheared single sheet test samples which are tested in accordance with ASTM test method A804. Induction is specified at 800 A/m. Induction grading is conducted using stress relief annealed Epstein samples tested in accordance with ASTM test method A343. Samples are secured from each end of the coil and the higher core loss and lower induction values are used for certification of conformance to product grade guarantees.

GUARANTEED CORE LOSS AND LAMINATION FACTOR

Product Name	Approximate Equivalent International Grade	Nominal Thickness, mm (in.)	Assumed Density, gm/cm³	Resistivity, Ω-m, x10⁻⁸	Maximum Core Loss Watts per kilogram		Maximum Core Loss Watts per pound		Minimum Induction at 800 A/m, T	Minimum Lamination Factor, %
					50 Hz		50 Hz			
					1.5 T	1.7 T	15 kg	17 kg		
M-3 CARLITE	M110-23S5	0.23 (0.009)	7.65	51	0.73	1.10	0.330	0.500	1.800	94.5%
M-4/120 CARLITE	M120-27S5	0.27 (0.011)			0.82	1.20	0.370	0.545	1.800	95.0%
M-4/125 CARLITE	M125-27S5	0.27 (0.011)			0.85	1.25	0.385	0.565	1.790	95.0%
M-5/125 CARLITE	M125-30S5	0.30 (0.012)			0.86	1.25	0.390	0.565	1.800	95.5%
M-5/130 CARLITE	M130-30S5	0.30 (0.012)			0.88	1.30	0.400	0.590	1.800	95.5%
M-5/140 CARLITE	M140-30S5	0.30 (0.012)			0.92	1.40	0.415	0.635	1.780	95.5%
M-6 CARLITE	M155-35S5	0.35 (0.014)			1.07	1.55	0.485	0.705	1.780	96.0%

TYPICAL CORE LOSS AND LAMINATION FACTOR

Product Name	Approximate Equivalent International Grade	Nominal Thickness, mm (in.)	Assumed Density, gm/cm³	Resistivity, Ω-m, x10⁻⁸	Typical Core Loss Watts per kilogram		Typical Core Loss Watts per pound		Typical Induction at 800 A/m, T	Typical Lamination Factor, %
					50 Hz		50 Hz			
					1.5 T	1.7 T	15 kg	17 kg		
M-3 CARLITE	M110-23S5	0.23 (0.009)	7.65	51	0.67	1.01	0.304	0.457	1.844	96.1%
M-4/120 CARLITE	M120-27S5	0.27 (0.011)			0.77	1.14	0.351	0.518	1.845	96.9%
M-4/125 CARLITE	M125-27S5	0.27 (0.011)			0.80	1.18	0.364	0.535	1.841	96.9%
M-5/125 CARLITE	M125-30S5	0.30 (0.012)			0.84	1.21	0.382	0.548	1.839	97.2%
M-5/130 CARLITE	M130-30S5	0.30 (0.012)			0.86	1.25	0.390	0.566	1.834	97.2%
M-5/140 CARLITE	M140-30S5	0.30 (0.012)			0.89	1.30	0.405	0.589	1.827	97.2%
M-6 CARLITE	M155-35S5	0.35 (0.014)			0.97	1.38	0.440	0.627	1.848	97.2%

The core loss and exciting power of the AK Steel TRAN-COR® H grades are determined by magnetic tests performed in accordance with general procedures approved by the American Society for Testing and Materials. The following conditions apply:

1. Results for as-sheared single sheet specimens from fully processed material cut parallel to the rolling direction of the coil and tested per ASTM A804
2. Density of all grades (7.65 gm/cm³) per ASTM A343

ASTM A664 is a grade identification system for electrical steels. While this system has not been widely adopted by the manufacturers and consumers of electrical steels, it is used in ASTM A876 to designate various grades of grain oriented electrical steel. The following is a listing of AK Steel and equivalent ASTM grades:

AK Steel grade M-3 is approximately equivalent to ASTM Core Loss Types 23G045 and 23H070, AK Steel grade M-4/125 is approximately equivalent to ASTM Core Loss Types 27G051 and 27H074, AK Steel grade M-5/140 is approximately equivalent to ASTM Core Loss Types 30G058 and 30H083, AK Steel grade M-6 is approximately equivalent to ASTM Core Loss Types 35G066 and 35H094

MANUFACTURING SPECIFICATIONS

Thickness	0.23 mm (0.009 in.) M-3 0.27 mm (0.011 in.) M-4 0.30 mm (0.012 in.) M-5 0.35 mm (0.014 in.) M-6	
Width	Master coils are available in widths of 914 mm (36.0 in.) and 920 mm (36.22 in.). For the 920 mm width, we reserve the option of furnishing cutdowns, in 900 mm (35.43 in.) and 880 mm (34.65 in.) widths, not to exceed 10% of the ordered quantity. For the 914 mm width, we reserve the option of furnishing cutdowns, in 890 mm (33.07 in.) and 870 mm (34.25 in.) widths, not to exceed 10% of the ordered quantity.	
Coils-Slit	Minimum width	19 mm (0.75 in.) Narrower - Inquire
	Inside diameters	406 mm (16.0 in.) 508 mm (20.0 in.)
Coils-Not Slit	Inside diameter	508 mm (20.0 in.)
Approximate Coil Weight	600 kg per 100 mm of width (335 lb per in. of width)	

TYPICAL VALUES OF CORE LOSS

AT 50 AND 60 Hz FOR TYPICAL SHEET SPECIMENS OF AK STEEL ORIENTED CARLITE COATED ELECTRICAL STEELS

	Core Loss (W/kg) - ASTM A804							
	0.23 mm M-3 CARLITE GOES		0.27 mm M-4/120 CARLITE GOES		0.27 mm M-4/125 CARLITE GOES		0.30 mm M-5/125 CARLITE GOES	
Flux Density (T)	50 Hz	60 Hz	50 Hz	60 Hz	50 Hz	60 Hz	50 Hz	60 Hz
0.1	0.00324	0.00424	0.00404	0.00533	0.00442	0.0058	0.00426	0.00567
0.2	0.0125	0.0164	0.0155	0.0205	0.0166	0.0219	0.0165	0.0219
0.3	0.0275	0.0360	0.0336	0.0444	0.0357	0.0470	0.0359	0.0478
0.4	0.0481	0.0629	0.0584	0.0765	0.0613	0.0805	0.0621	0.0827
0.5	0.0740	0.0965	0.0882	0.116	0.0928	0.122	0.0948	0.126
0.6	0.105	0.137	0.124	0.164	0.130	0.171	0.134	0.178
0.7	0.141	0.184	0.166	0.218	0.173	0.227	0.180	0.238
0.8	0.183	0.238	0.213	0.281	0.222	0.292	0.232	0.307
0.9	0.229	0.298	0.267	0.351	0.278	0.365	0.291	0.385
1.0	0.281	0.366	0.327	0.430	0.340	0.447	0.358	0.473
1.1	0.339	0.441	0.395	0.519	0.410	0.539	0.432	0.570
1.2	0.404	0.525	0.471	0.620	0.489	0.642	0.515	0.680
1.3	0.477	0.621	0.558	0.734	0.580	0.760	0.608	0.803
1.4	0.562	0.731	0.657	0.863	0.682	0.893	0.714	0.942
1.5	0.668	0.866	0.778	1.02	0.806	1.05	0.842	1.11
1.6	0.799	1.03	0.921	1.20	0.955	1.24	0.993	1.30
1.7	1.00	1.28	1.13	1.47	1.18	1.52	1.21	1.57
1.8	1.34	1.70	1.45	1.86	1.51	1.94	1.53	1.98
1.9	1.75	2.20	1.70	2.18	1.91	2.42	1.92	2.45

	Core Loss (W/kg) - ASTM A804					
	0.30 mm M-5/130 CARLITE GOES		0.30 mm M-5/140 CARLITE GOES		0.35 mm M-6 CARLITE GOES	
Flux Density (T)	50 Hz	60 Hz	50 Hz	60 Hz	50 Hz	60 Hz
0.1	0.00430	0.00572	0.00473	0.00629	0.00544	0.00725
0.2	0.0167	0.0222	0.0180	0.0240	0.0205	0.0274
0.3	0.0364	0.0485	0.0389	0.0519	0.0439	0.0589
0.4	0.0630	0.0839	0.0669	0.0892	0.0753	0.101
0.5	0.0963	0.128	0.102	0.135	0.114	0.153
0.6	0.136	0.181	0.143	0.190	0.160	0.214
0.7	0.183	0.242	0.191	0.253	0.214	0.286
0.8	0.236	0.312	0.246	0.326	0.275	0.367
0.9	0.296	0.392	0.308	0.408	0.344	0.458
1.0	0.364	0.481	0.378	0.500	0.421	0.560
1.1	0.439	0.580	0.456	0.602	0.507	0.673
1.2	0.524	0.692	0.543	0.718	0.602	0.799
1.3	0.620	0.818	0.643	0.849	0.709	0.940
1.4	0.728	0.960	0.756	0.997	0.829	1.10
1.5	0.860	1.13	0.894	1.18	0.970	1.28
1.6	1.02	1.33	1.06	1.39	1.14	1.51
1.7	1.25	1.62	1.30	1.69	1.38	1.81
1.8	1.59	2.05	1.66	2.14	1.71	2.24
1.9	1.98	2.54	2.07	2.66	2.03	2.62

TYPICAL VALUES OF RMS EXCITING POWER

AT 50 AND 60 Hz FOR TYPICAL SHEET SPECIMENS OF AK STEEL ORIENTED CARLITE COATED ELECTRICAL STEELS

	Exciting Power (rms VA/kg) - ASTM A804							
	0.23 mm M-3 CARLITE GOES		0.27 mm M-4/120 CARLITE GOES		0.27 mm M-4/125 CARLITE GOES		0.30 mm M-5/125 CARLITE GOES	
Flux Density (T)	50 Hz	60 Hz	50 Hz	60 Hz	50 Hz	60 Hz	50 Hz	60 Hz
0.1	0.0101	0.0123	0.0104	0.0129	0.0109	0.0134	0.00918	0.0114
0.2	0.0334	0.0411	0.0340	0.0424	0.0354	0.0440	0.0302	0.0380
0.3	0.0662	0.0814	0.0671	0.0840	0.0693	0.0867	0.0603	0.0762
0.4	0.106	0.131	0.108	0.135	0.111	0.139	0.0978	0.124
0.5	0.151	0.187	0.154	0.194	0.158	0.199	0.142	0.181
0.6	0.201	0.249	0.206	0.261	0.212	0.267	0.193	0.246
0.7	0.256	0.318	0.265	0.335	0.270	0.342	0.250	0.320
0.8	0.316	0.394	0.329	0.417	0.335	0.425	0.314	0.403
0.9	0.382	0.478	0.400	0.509	0.407	0.517	0.386	0.495
1.0	0.457	0.572	0.480	0.611	0.487	0.620	0.467	0.600
1.1	0.538	0.674	0.569	0.725	0.577	0.734	0.558	0.717
1.2	0.634	0.794	0.674	0.857	0.681	0.867	0.666	0.854
1.3	0.757	0.946	0.804	1.02	0.811	1.03	0.799	1.02
1.4	0.905	1.13	0.964	1.22	0.969	1.23	0.971	1.24
1.5	1.15	1.42	1.22	1.53	1.22	1.53	1.22	1.54
1.6	1.51	1.86	1.57	1.95	1.57	1.95	1.61	2.01
1.7	2.64	3.19	2.75	3.36	2.78	3.38	2.87	3.51
1.8	7.04	8.47	7.71	9.36	8.05	9.64	8.03	9.76
1.9	25.9	31.1	27.3	33.3	28.8	34.4	27.9	34.1

	Exciting Power (rms VA/kg) - ASTM A804					
	0.30 mm M-5/130 CARLITE GOES		0.30 mm M-5/140 CARLITE GOES		0.35 mm M-6 CARLITE GOES	
Flux Density (T)	50 Hz	60 Hz	50 Hz	60 Hz	50 Hz	60 Hz
0.1	0.00922	0.0115	0.0105	0.0131	0.00895	0.0114
0.2	0.0304	0.0383	0.0341	0.0430	0.0296	0.0381
0.3	0.0607	0.0768	0.0675	0.0852	0.0595	0.0771
0.4	0.0985	0.125	0.108	0.138	0.0977	0.127
0.5	0.143	0.182	0.157	0.199	0.144	0.187
0.6	0.194	0.248	0.211	0.270	0.197	0.257
0.7	0.252	0.323	0.273	0.349	0.257	0.336
0.8	0.317	0.407	0.341	0.438	0.326	0.426
0.9	0.391	0.502	0.419	0.538	0.403	0.527
1.0	0.474	0.609	0.506	0.650	0.490	0.639
1.1	0.569	0.730	0.605	0.777	0.587	0.767
1.2	0.681	0.872	0.723	0.926	0.700	0.913
1.3	0.821	1.05	0.870	1.11	0.836	1.09
1.4	1.01	1.28	1.07	1.35	1.01	1.30
1.5	1.28	1.62	1.36	1.71	1.26	1.62
1.6	1.73	2.15	1.83	2.28	1.68	2.13
1.7	3.20	3.92	3.43	4.20	3.05	3.76
1.8	9.06	11.0	9.66	11.7	9.18	11.0
1.9	30.4	37.1	31.6	38.7	33.5	40.1

CORE LOSS CURVE – M-4/120 CARLITE

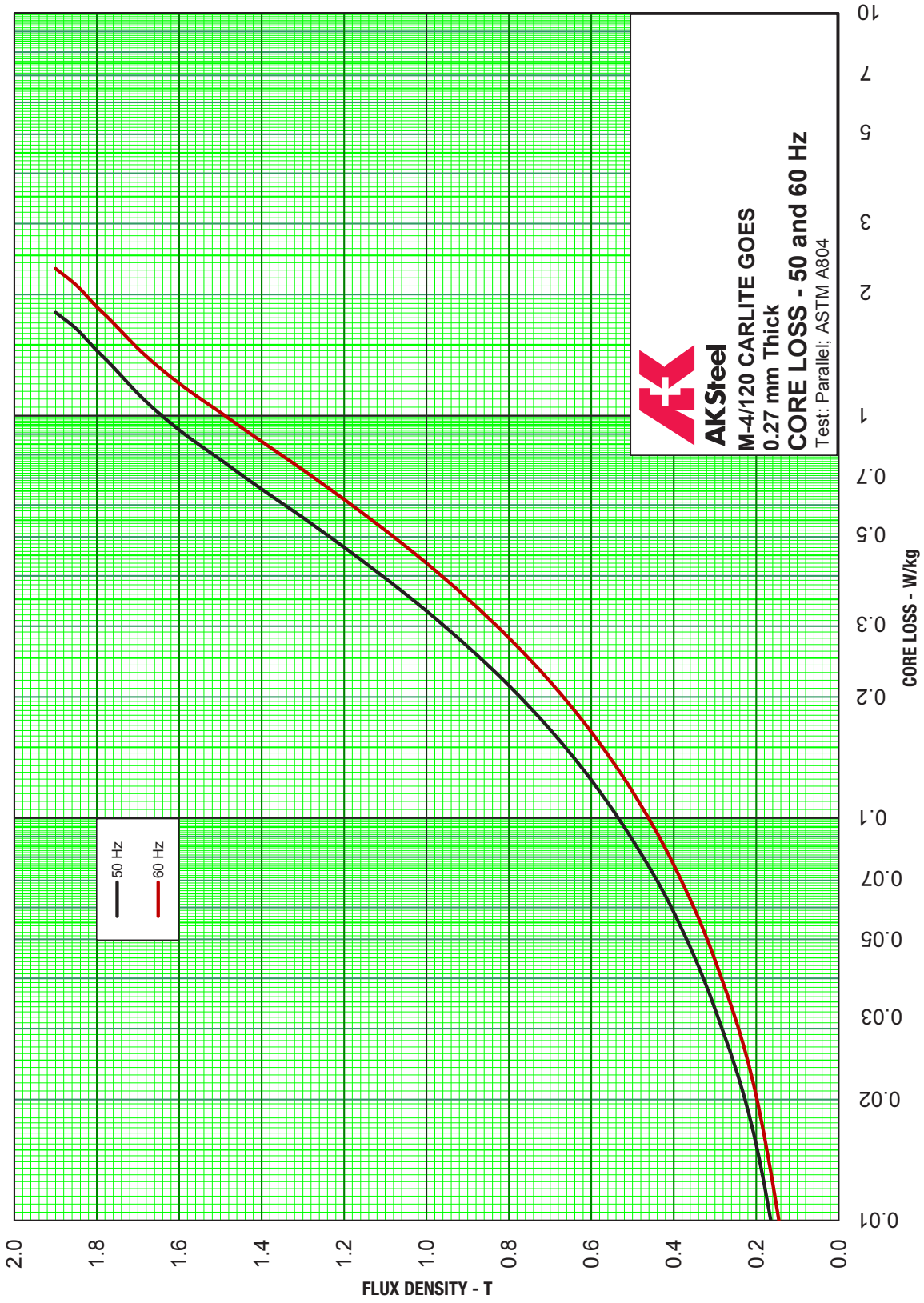

EXCITING POWER CURVE – M-4/120 CARLITE

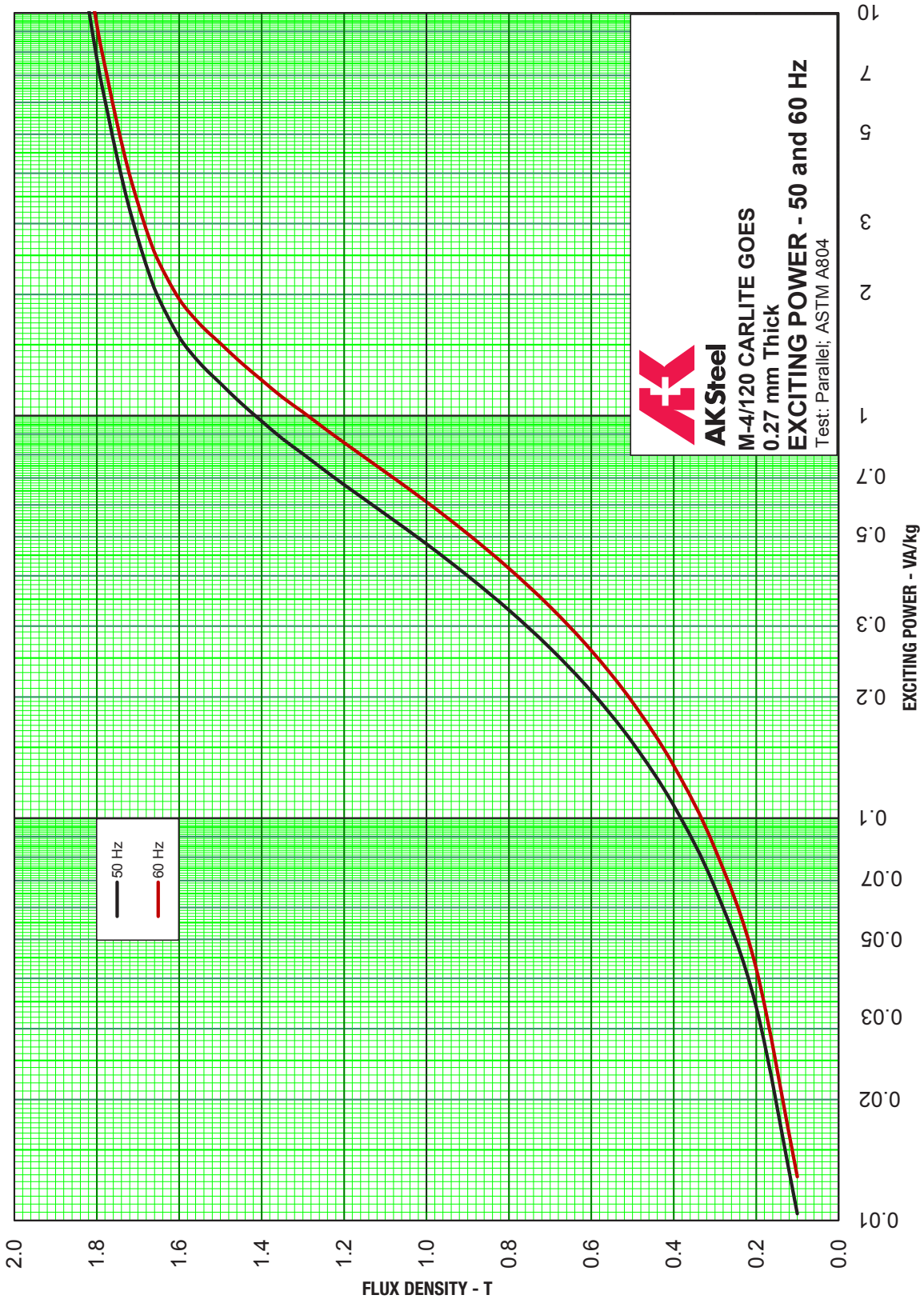

D-C MAGNETIZATION CURVE – M-4/120 CARLITE

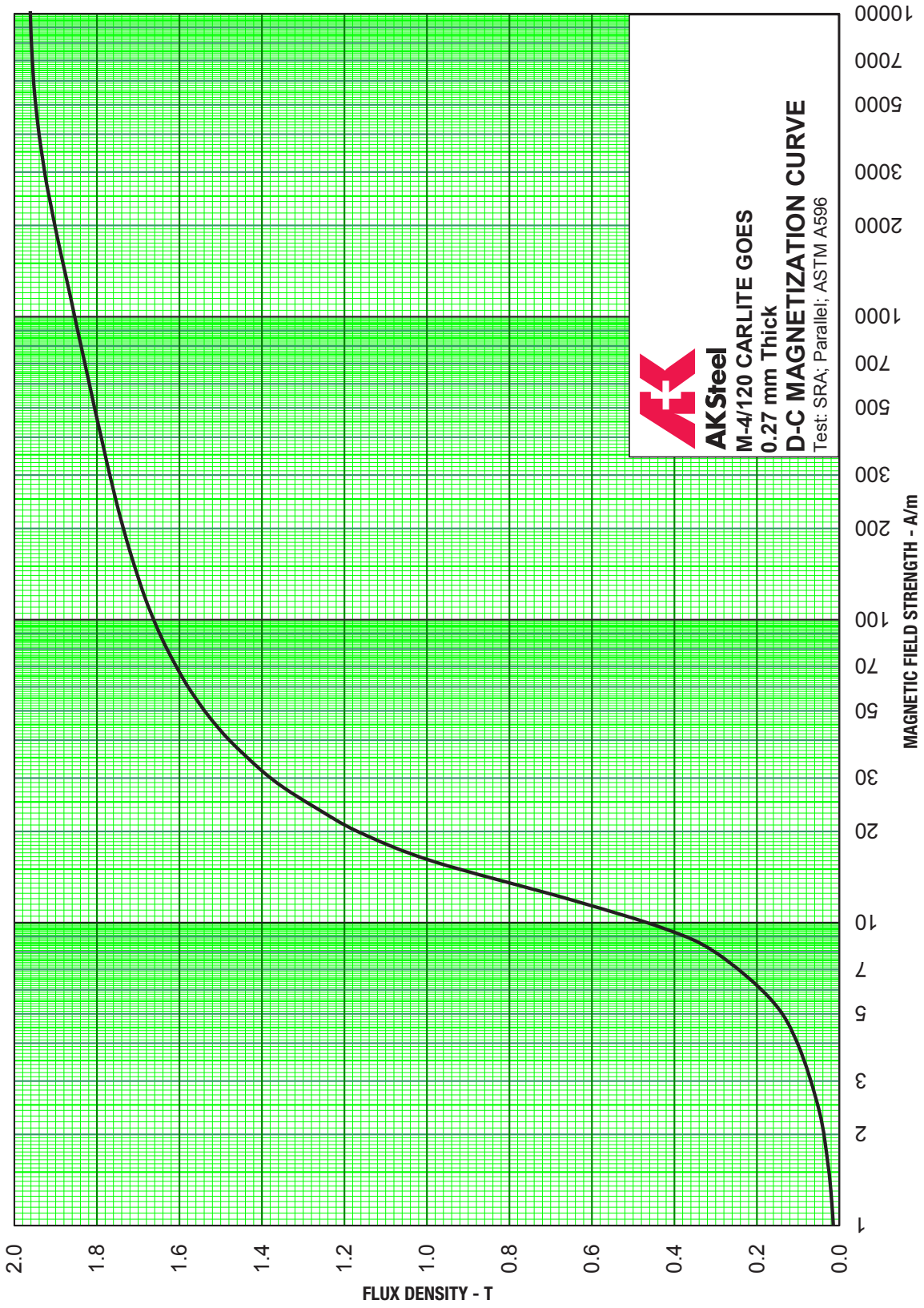

D-C HYSTERESIS LOOPS – M-4/120 CARLITE